

# ニュートリノ中性カレント反応理解のための 中性子・酸素原子核反応に関する研究

Study of neutron-oxygen reaction  
for understanding neutral current interaction

Okayama Univ.  
Tomohiro Tano

10th Supernova Neutrino Workshop @Okayama Univ.  
Feb. 29 - Mar. 1, 2024

# Outline

1. Introduction
2. Measurement of neutron-oxygen reaction
3. Analysis
4. Discussion
5. Summary

# SK-Gd experiment

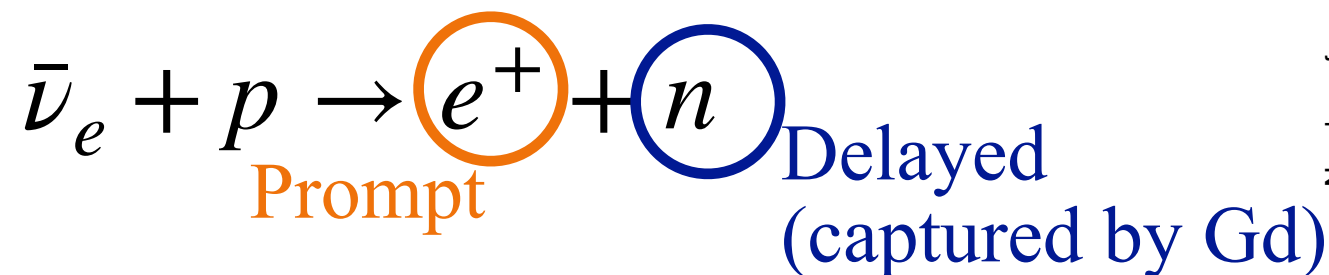
3

# Loading Gadolinium in SK

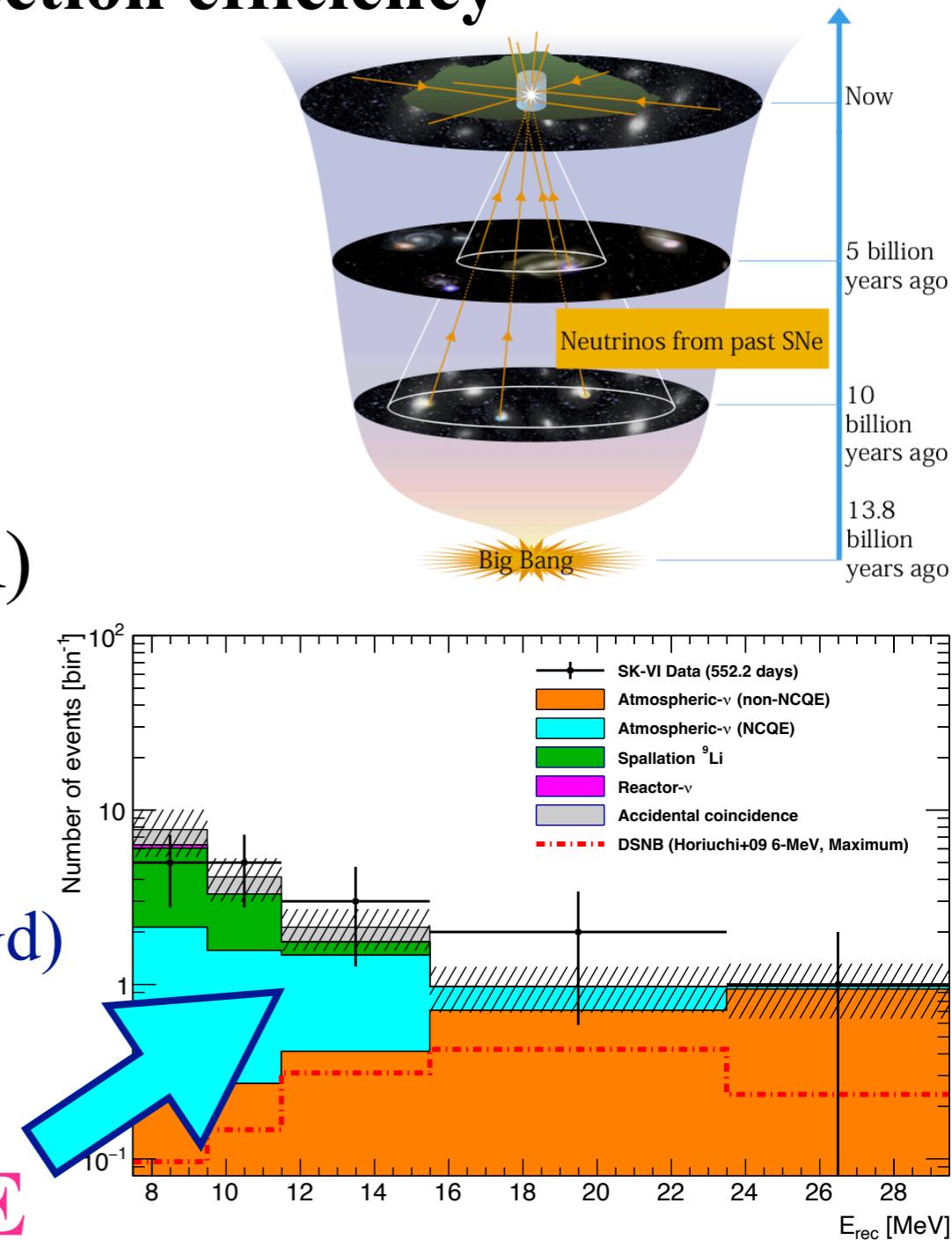


# Improvement of neutron detection efficiency

- Supernova Relic Neutrino (DSNB)
    - ▶ Integrated neutrino flux from all of supernova in the past
    - ▶ Star formation history
  - DSNB search in Super-Kamiokande (SK)
    - ▶ Inverse beta decay (IBD) events

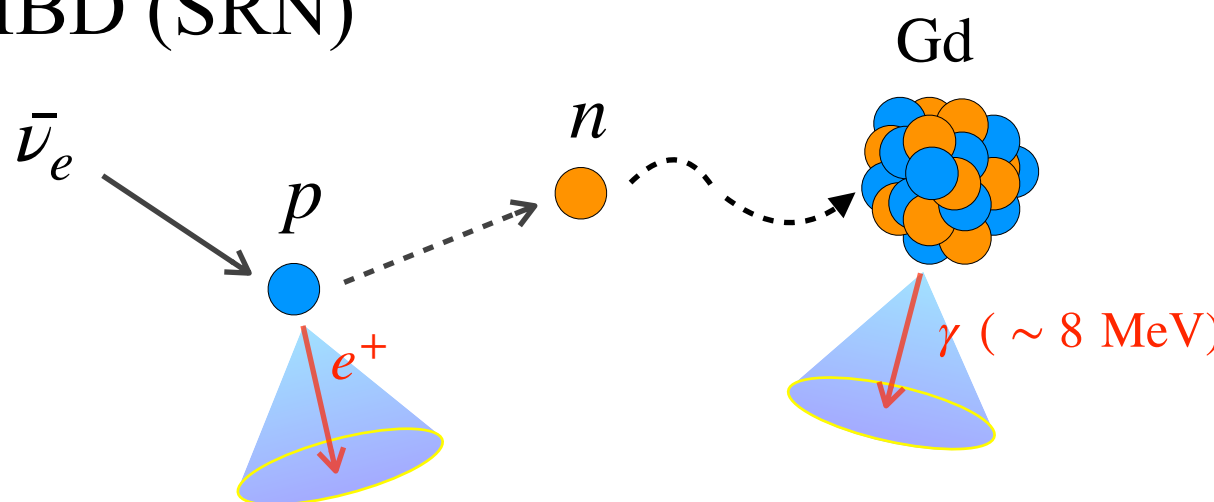


- Neutral current quasi-elastic scattering by atmospheric neutrino is the largest background

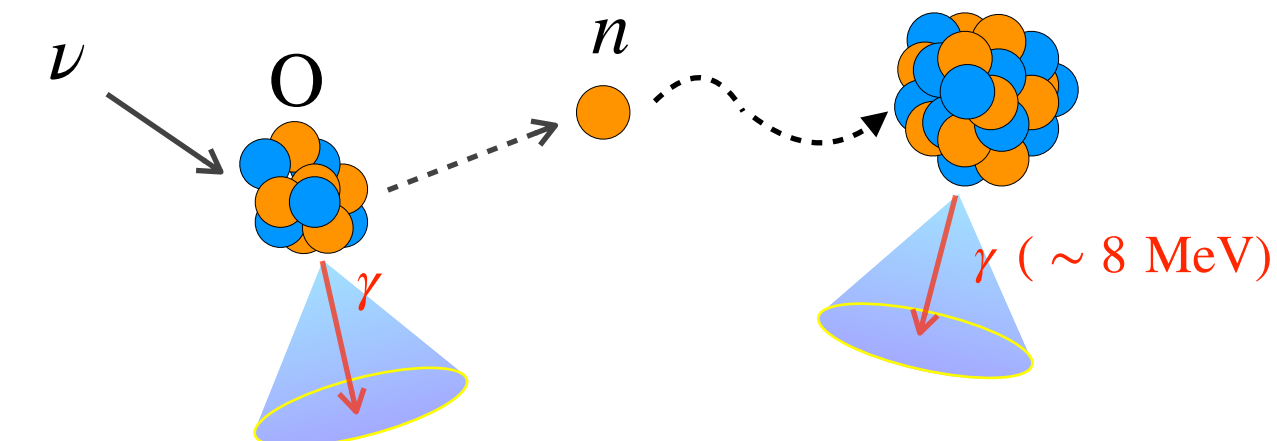


# NCQE interaction

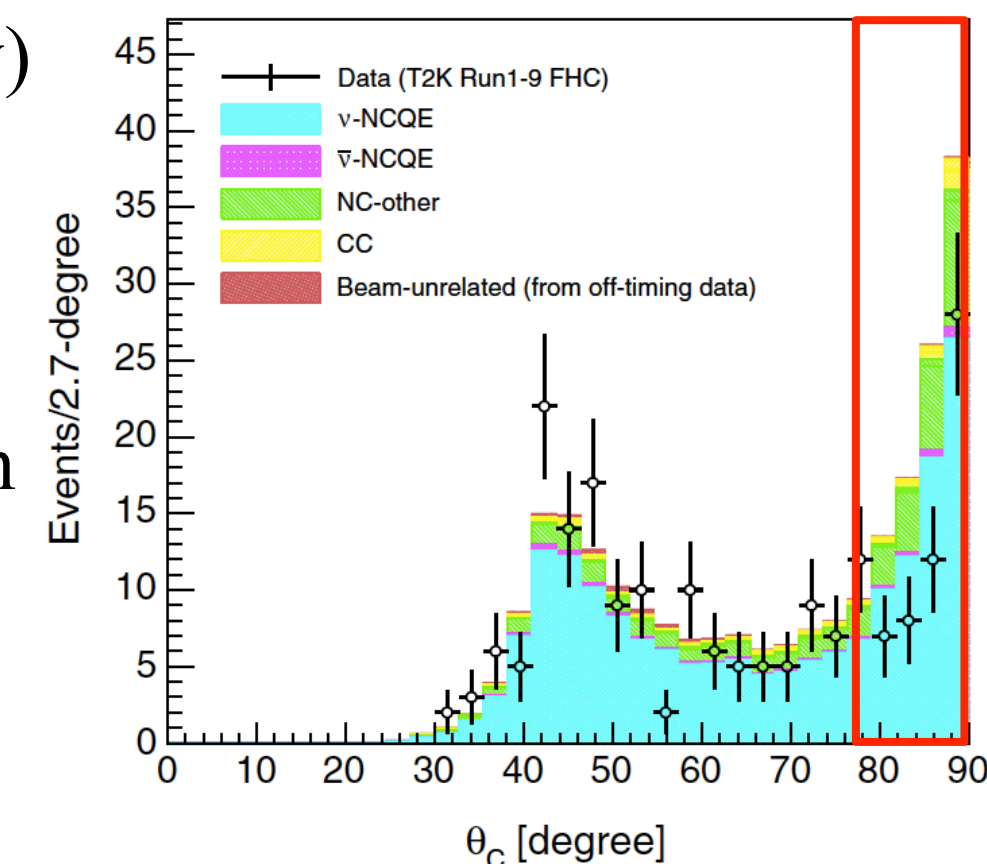
IBD (SRN)



NCQE (atm. v)

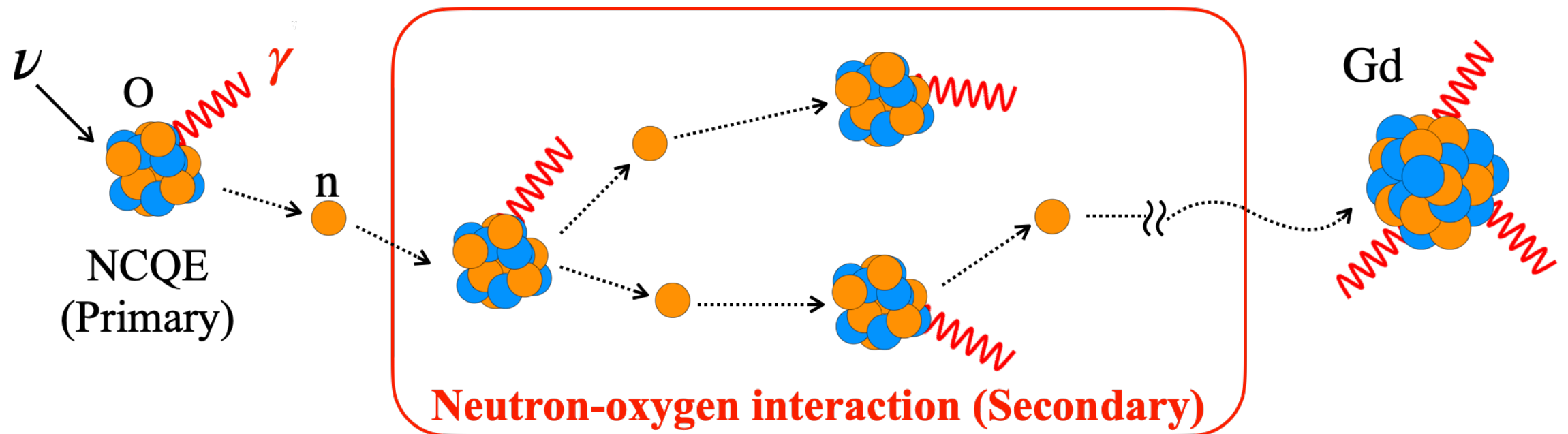


- NCQE events cannot be distinguished from IBD
- The number of NCQE events is estimated by simulation
  - ▶ Systematic error : 68 - 82% (largest uncertainty)
- Measurement of NCQE interaction using T2K neutrino beam
  - ▶ Cherenkov angle distribution has differences b/w data and MC expected at large angle region
  - ▶ Caused by  $\gamma$ -rays from neutron- $^{16}\text{O}$  interaction (described in the next page)

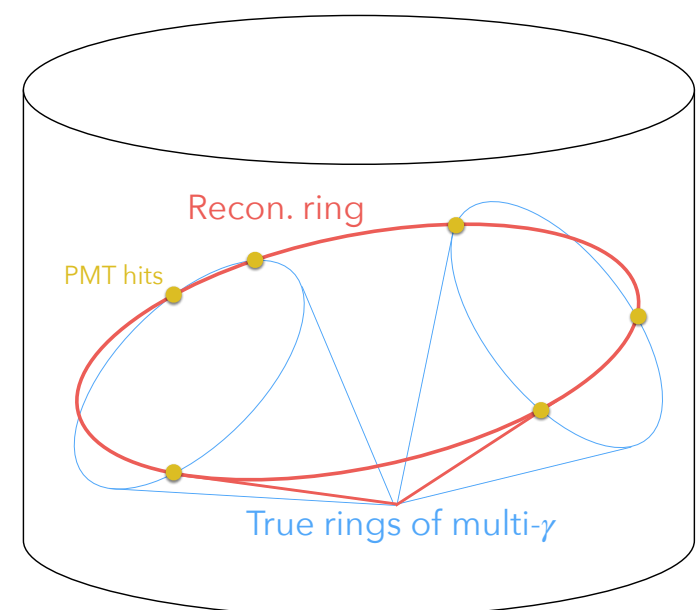


# Neutron- $^{16}\text{O}$ interaction

5



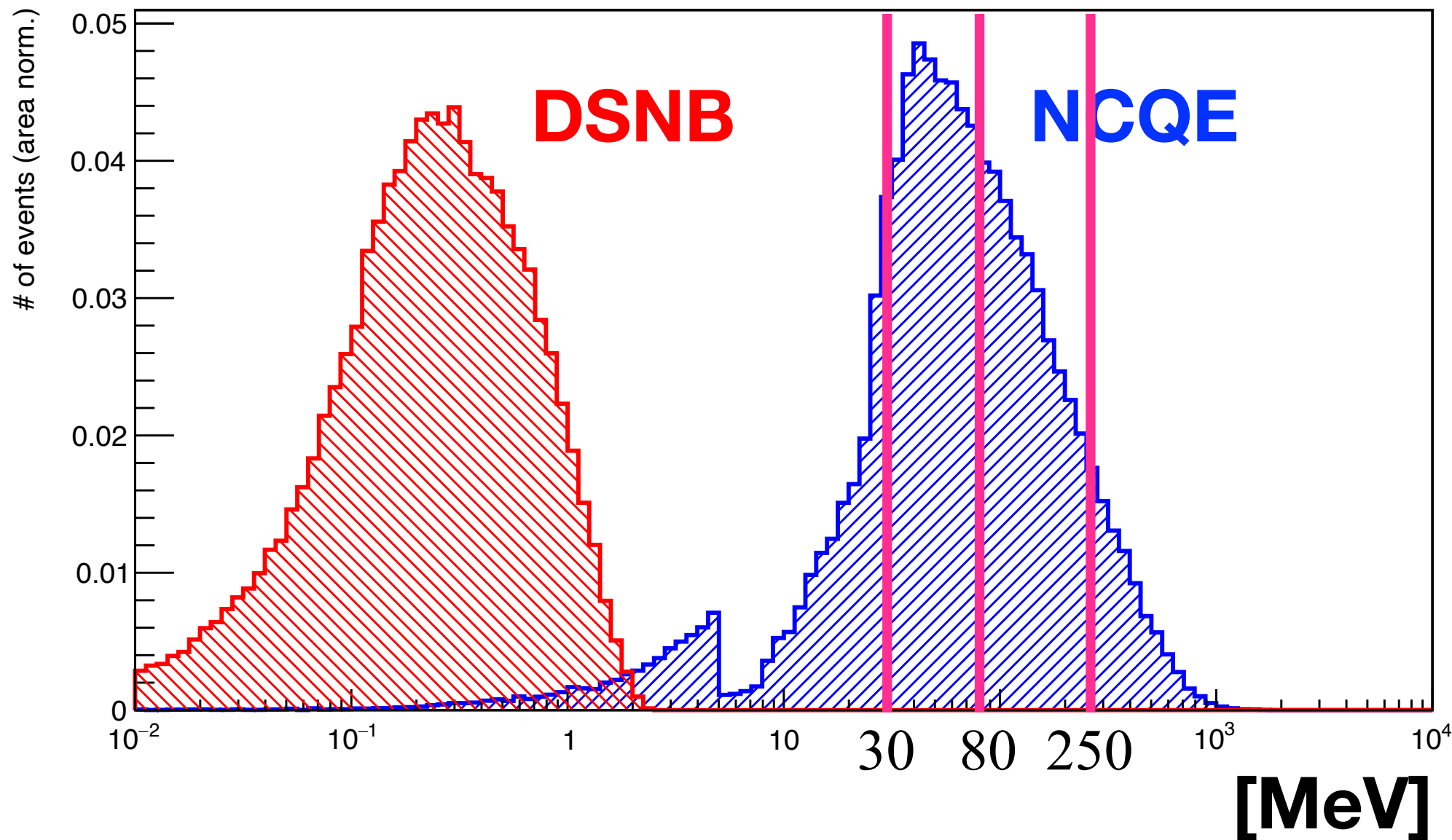
- Primary  $\gamma$  :  $\gamma$ -rays from NCQE
- Secondary  $\gamma$  :  $\gamma$ -rays from neutron emitted by NCQE with oxygen nucleus
- Primary and secondary  $\gamma$ -rays are detected as one Cherenkov ring  
→ Reconstructed Cherenkov angle is large
- Neutron interaction with oxygen are poorly understood and the cause of uncertainty



**It is important to understand neutron- $^{16}\text{O}$  reaction**

# Neutrons emitted by NCQE

- Energies of neutrons emitted by NCQE are  $\mathcal{O}(10^1) \sim \mathcal{O}(10^2)$  MeV
- We measured neutron interaction with  $^{16}\text{O}$  at 30, 80, 250 MeV for covering this energy range

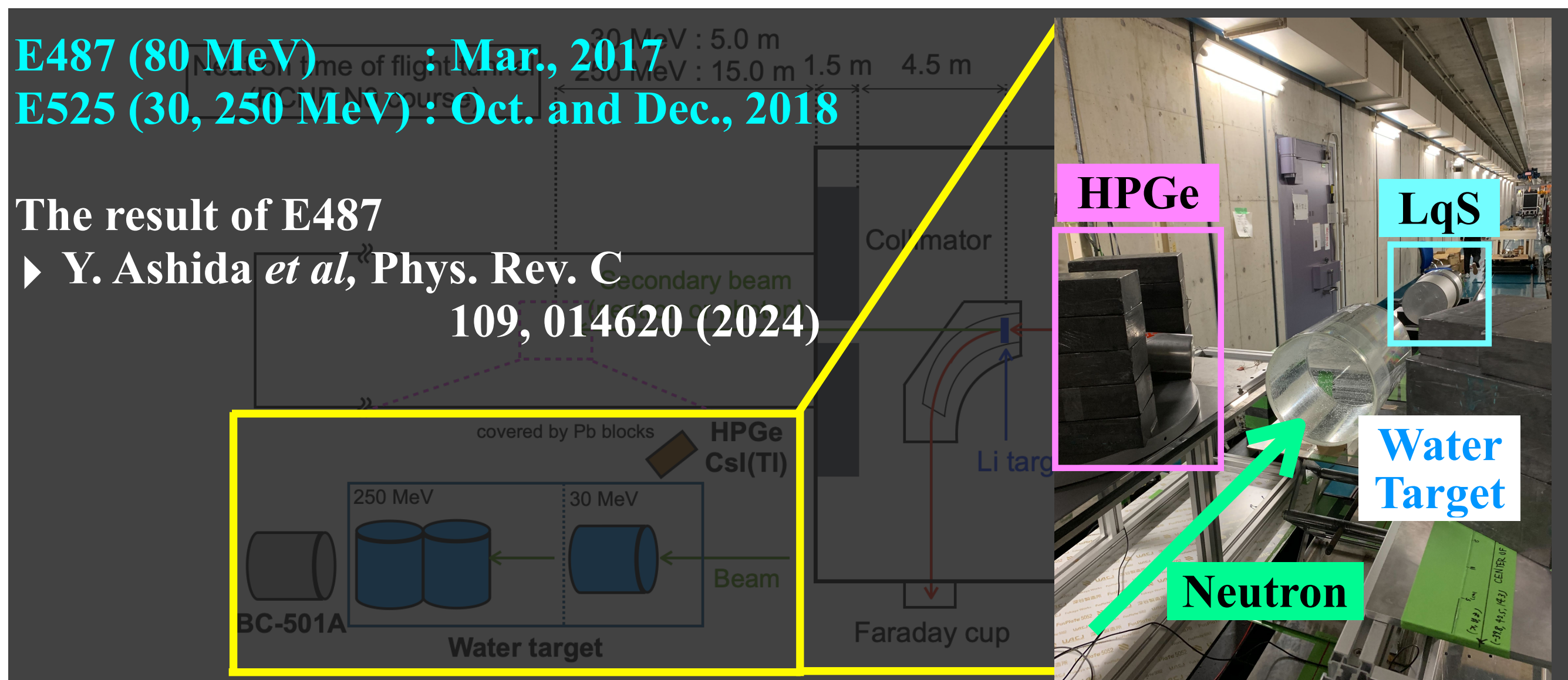


# Experiment @Research Center for Nuclear Physics

7

- Neutrons were made incident on water target and interacts with  $^{16}\text{O}$
- $\gamma$ -rays produced by neutron- $^{16}\text{O}$  reaction were measured

Energy	Neutron detector	Gamma-rays Detector
30 MeV	LqS	HPGe
80 MeV	LqS	$\text{LaBr}_3$
250 MeV	LqS	HPGe



# Cross section extraction

$$\text{Cross Section} = \frac{\text{Number of } \gamma\text{-rays}}{\text{Number of incident neutrons}}$$

**Number of incident neutrons**  
are estimated by LqS data

Neutron selection

Energy reconstruction

Detection efficiency  
estimation

Neutron flux

**Number of**  $\gamma$ **-rays**  
are estimated by HPGe data

Energy calibration

Background subtraction

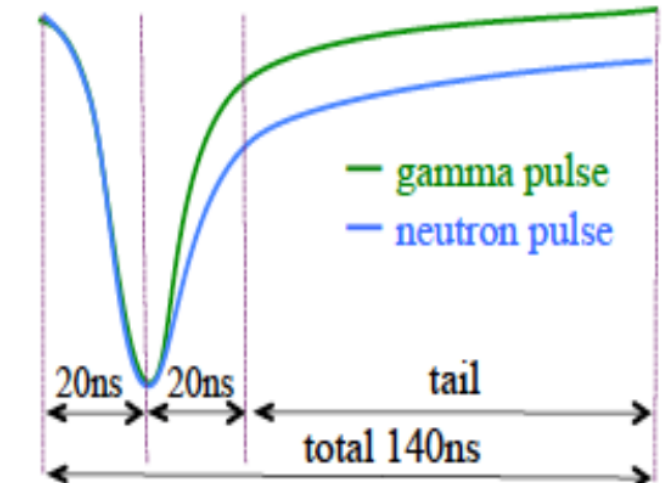
Spectrum fitting

$\gamma$ -rays intensity

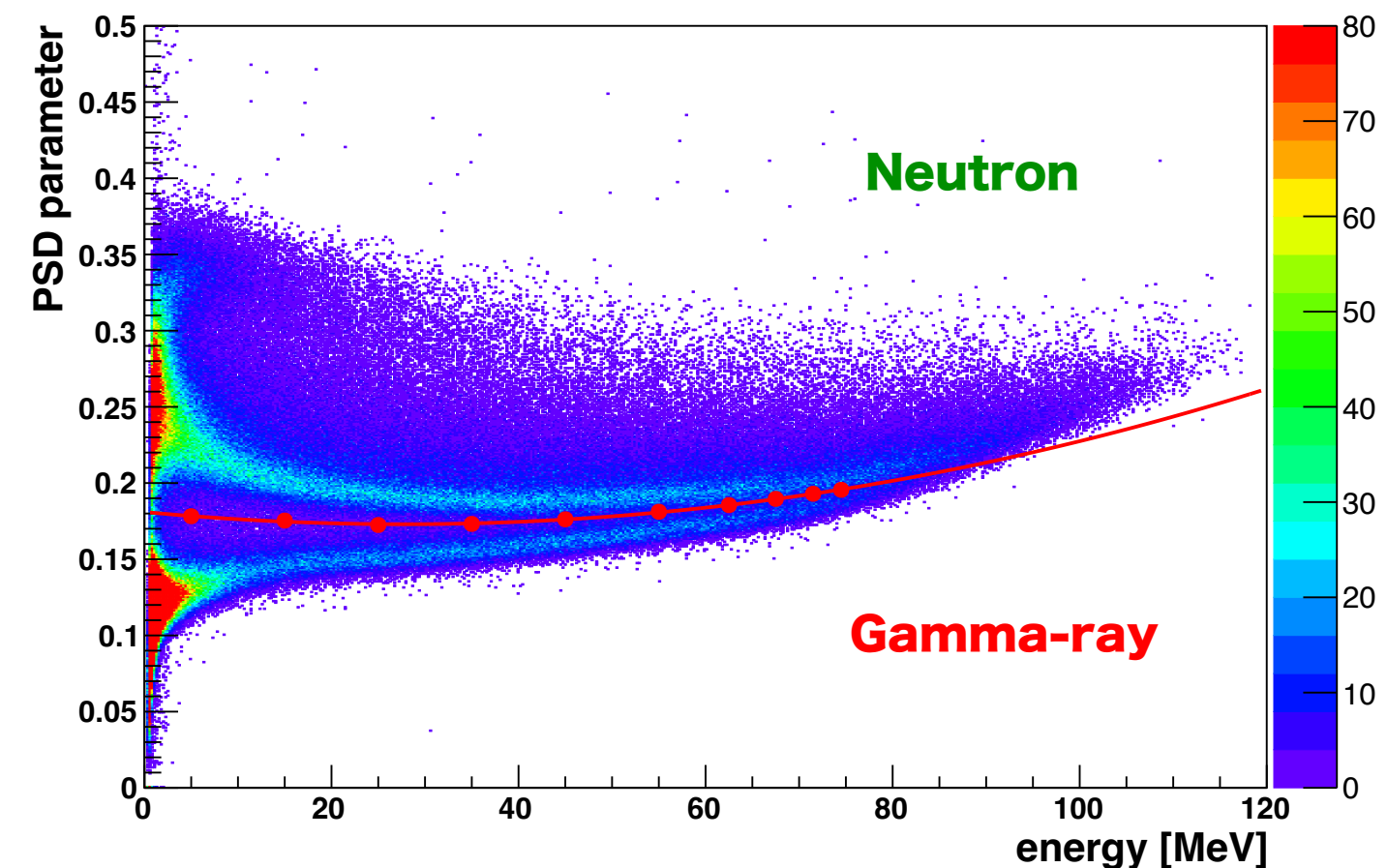
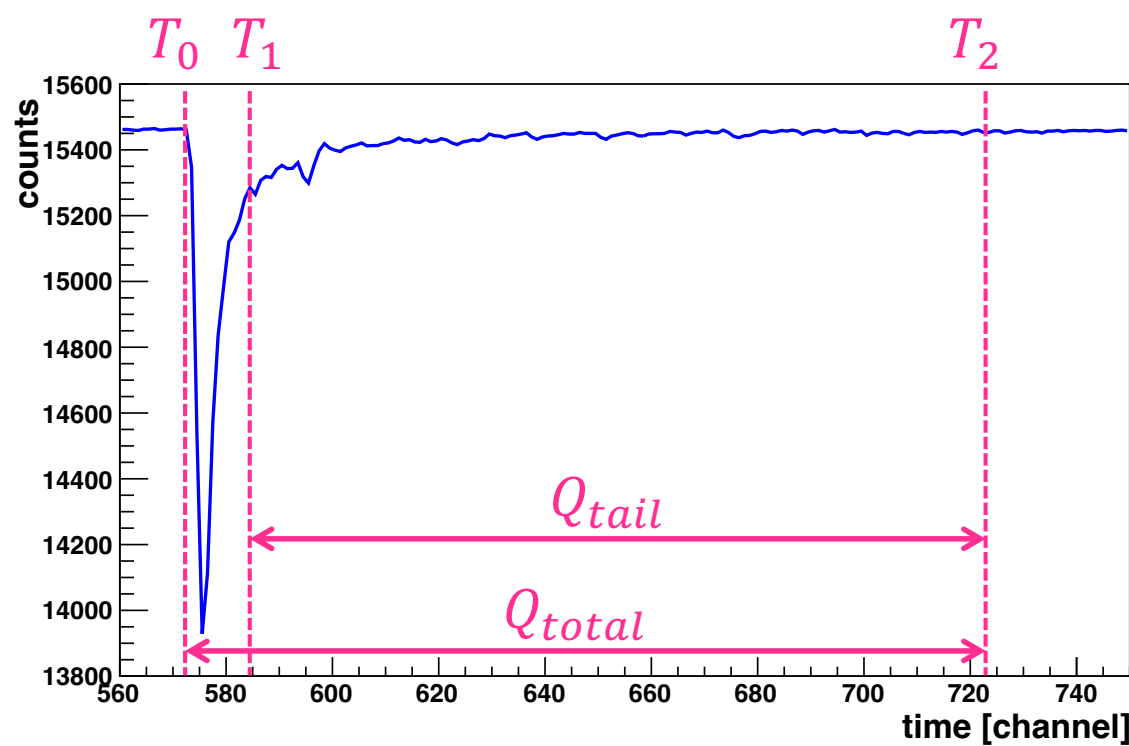
# Neutron selection

- Neutron-like events are selected using Pulse Shape Discrimination (PSD)

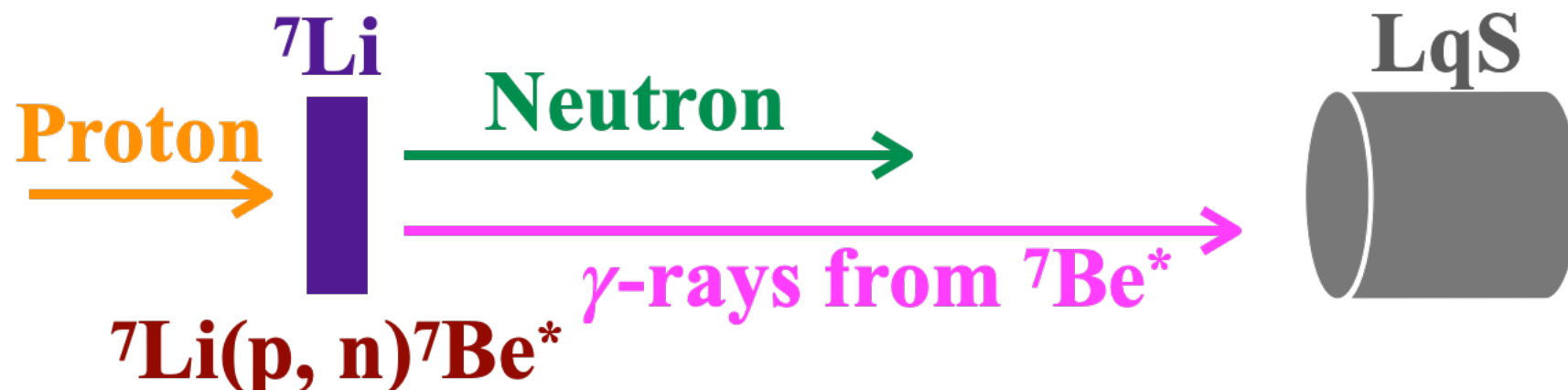
$$\text{PSD parameter} = \frac{Q_{\text{tail}}}{Q_{\text{total}}}$$



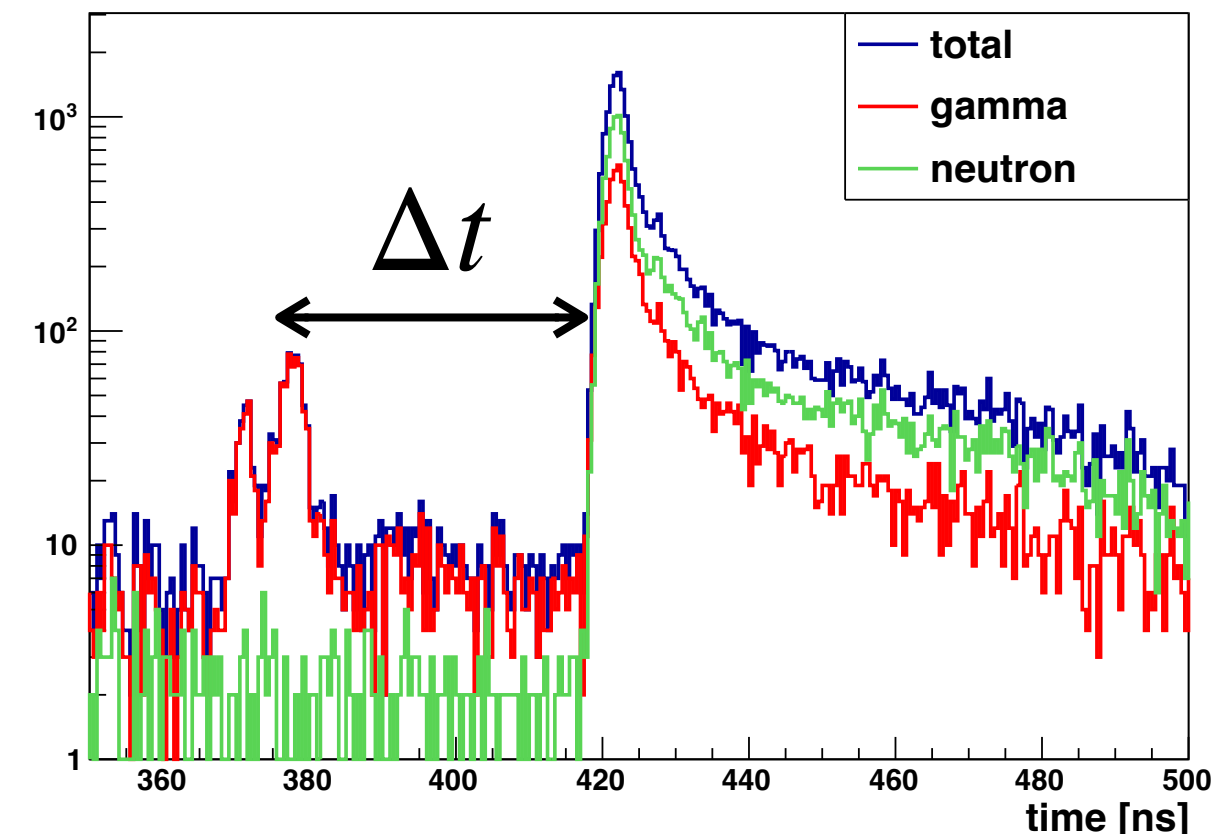
- Waveforms of n-like events have longer tail, larger PSD parameter
- Cut criteria were determined for each energy region



# Energy reconstruction



- Neutrons are generated by  ${}^7\text{Li}(\text{p}, \text{n}){}^7\text{Be}^*$
- Flash gamma :  $\gamma$ -rays from  $\text{Be}^*$
- Neutron energy was calculated based on time difference b/w flash gamma and neutron

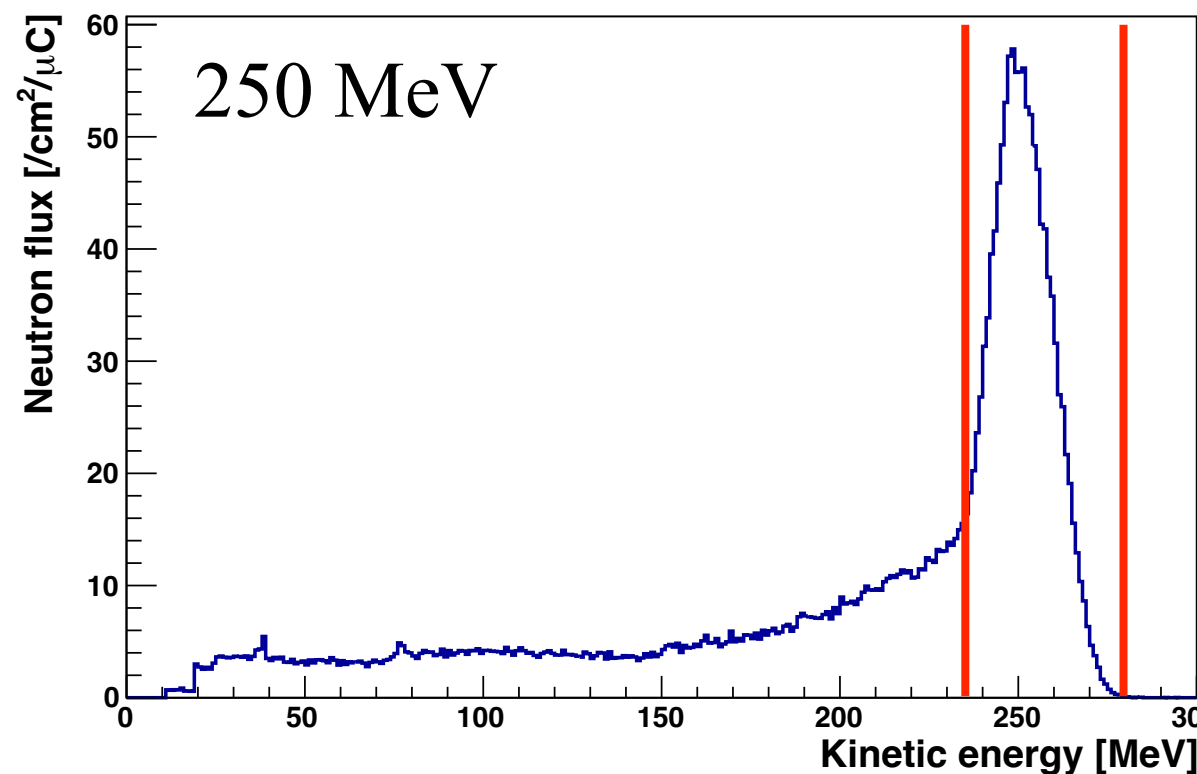
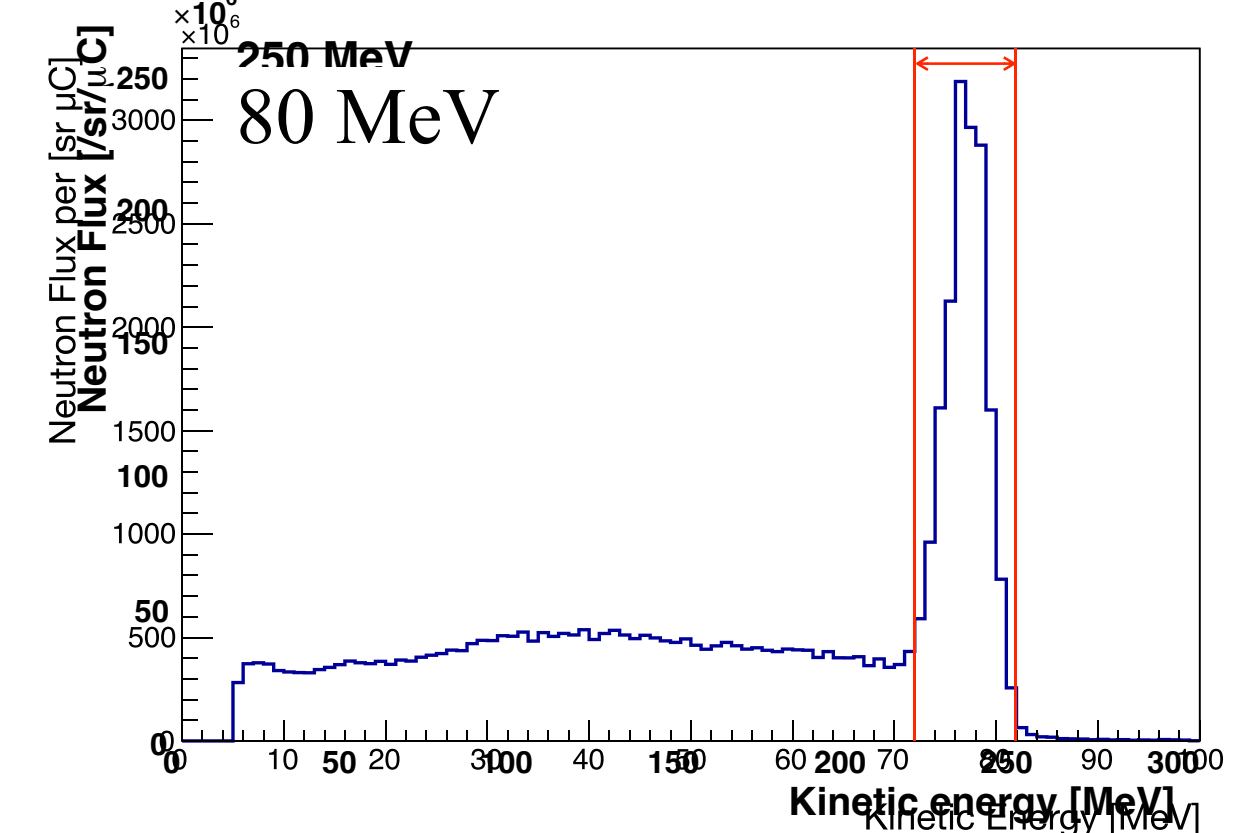
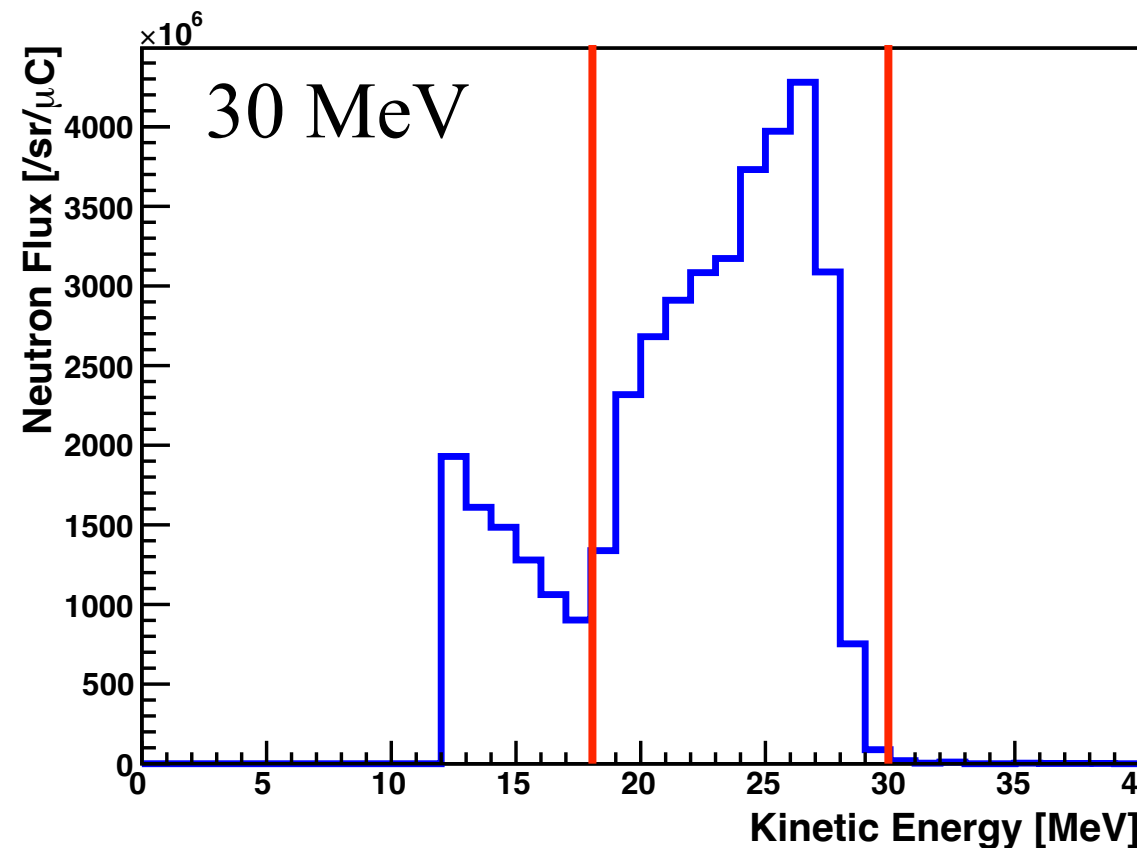


$$K = \frac{mc^2}{\sqrt{1 - \left(\frac{1}{1 + \frac{c}{L}}\Delta t\right)^2}} - mc^2$$

mc<sup>2</sup> : Neutron mass (939.6 MeV)  
 L : Distance from Li to water  
 Δt : Time difference

# Neutron flux

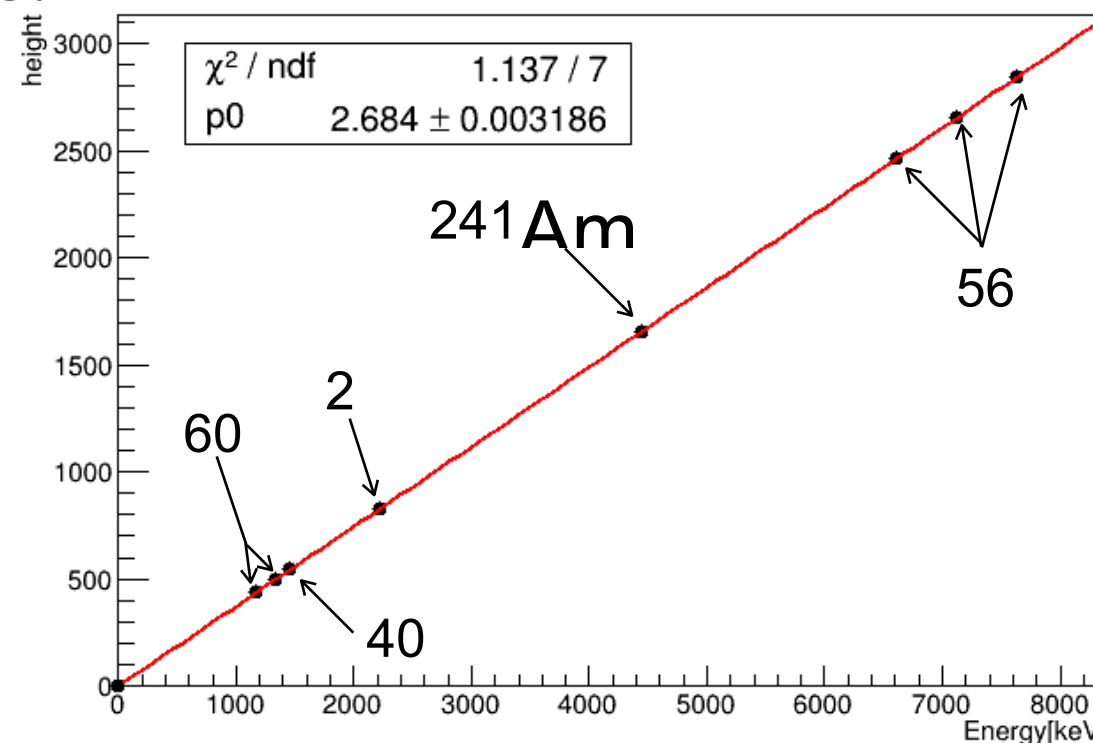
11



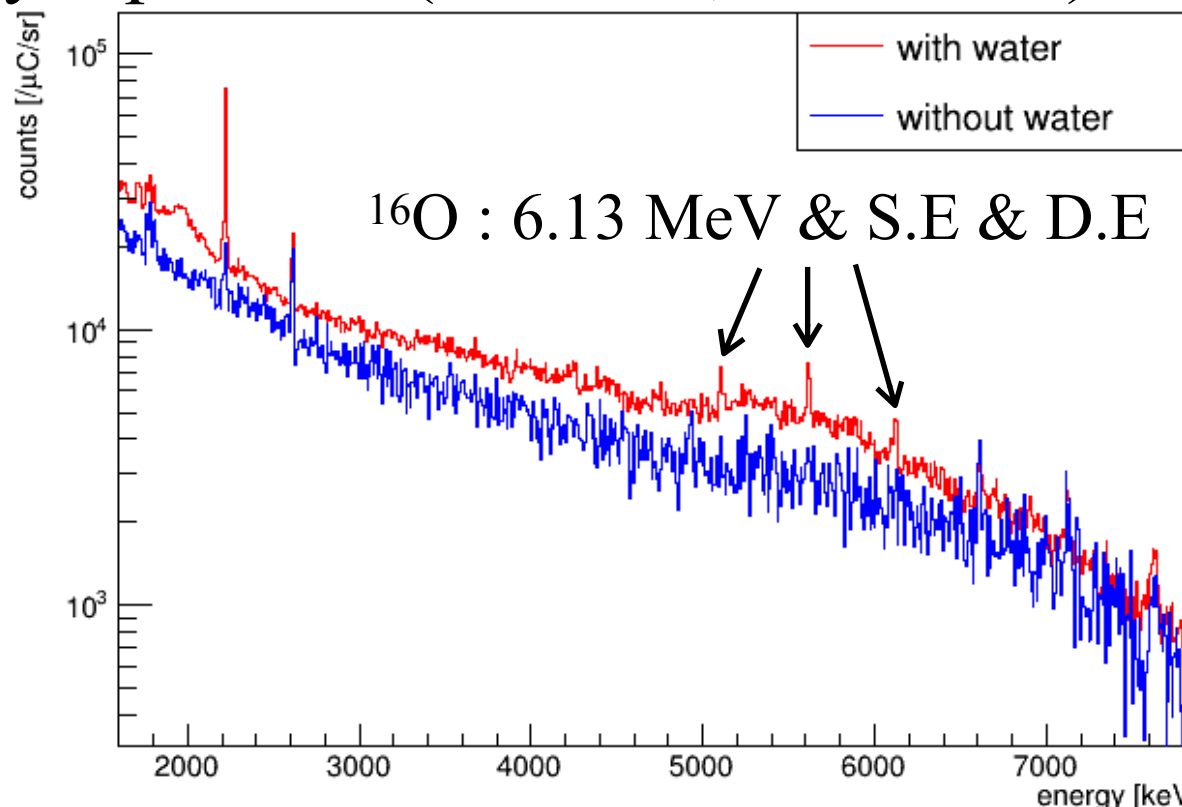
- Neutron flux for 30, 80, 250 MeV experiment have consistency with previous study (Y. Iwamoto *et al.*, 2015)

# Gamma-rays analysis

## Energy calibration



## $\gamma$ -rays spectrum (w/ water, w/o water)



Energy calibration

Background subtraction

Spectrum fitting

$\gamma$ -rays intensity

- Linearity was confirmed (< 1%)
- $\gamma$ -rays peak from  $^{16}\text{O}$  (6.13 MeV) is seen in w/ water spectrum

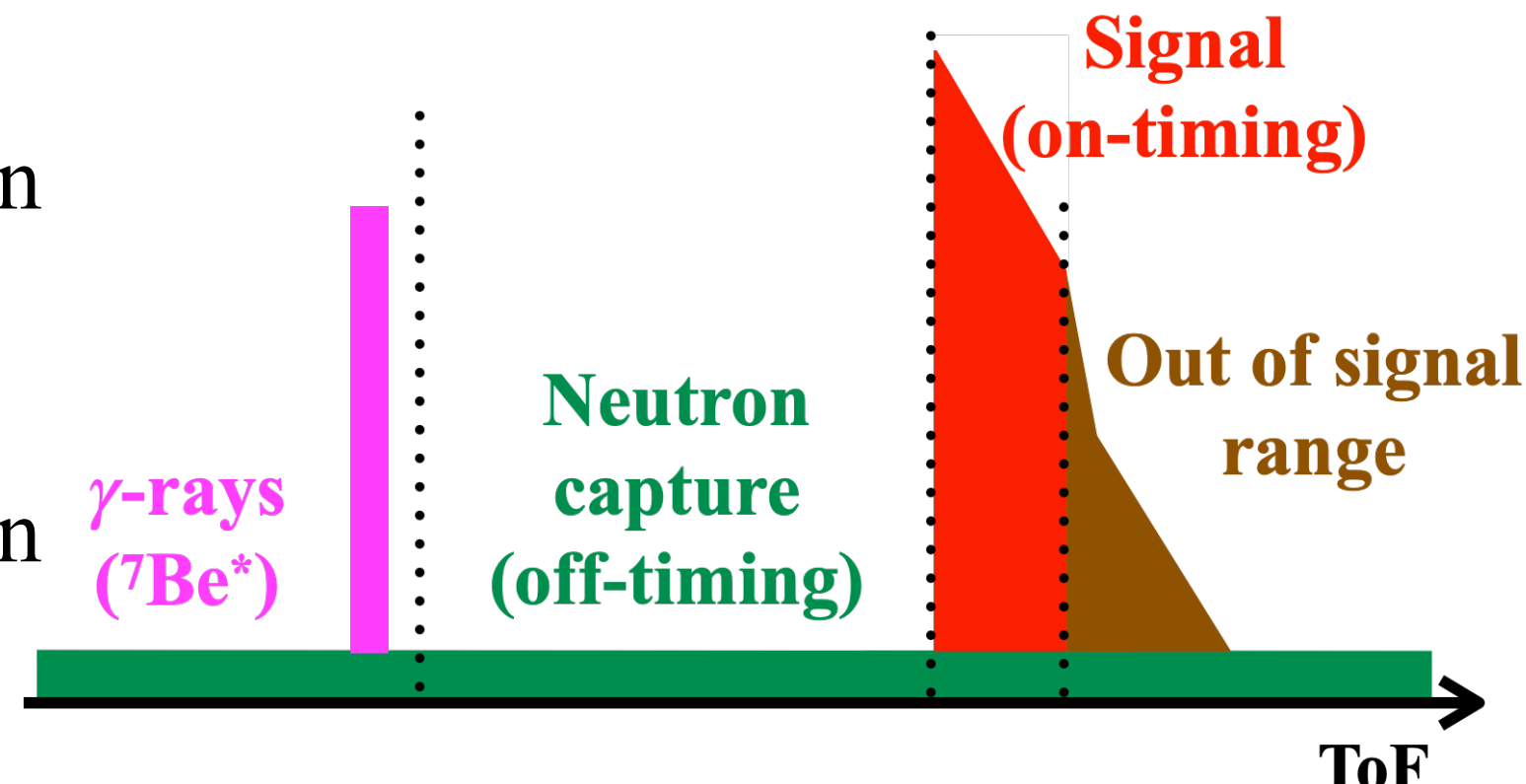
# Background subtraction

## Signal

- Neutron -  $^{16}\text{O}$  interaction  
(235-270 MeV)

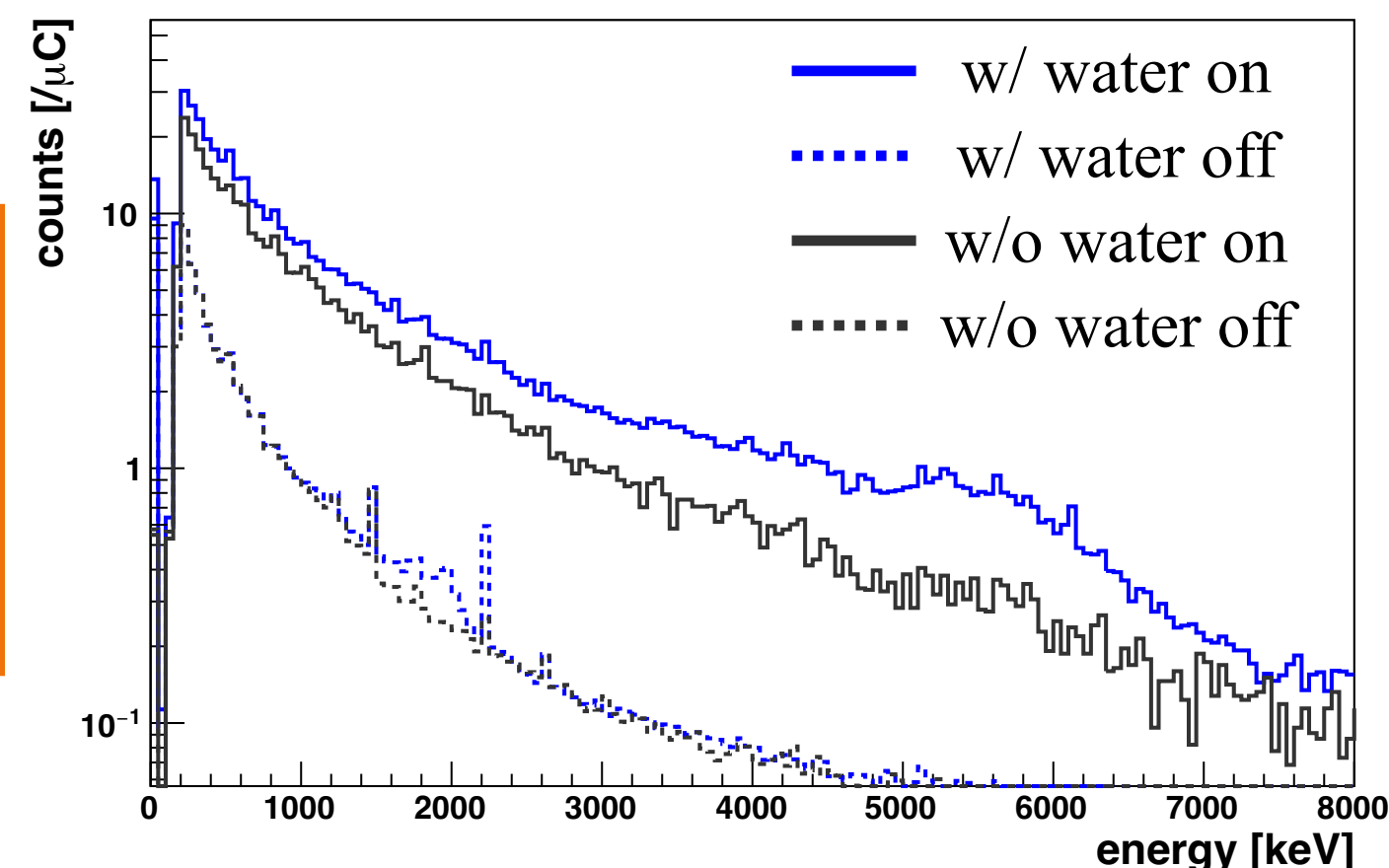
## Background

- Neutron -  $^{16}\text{O}$  interaction  
(below 235 MeV)
- Neutron capture



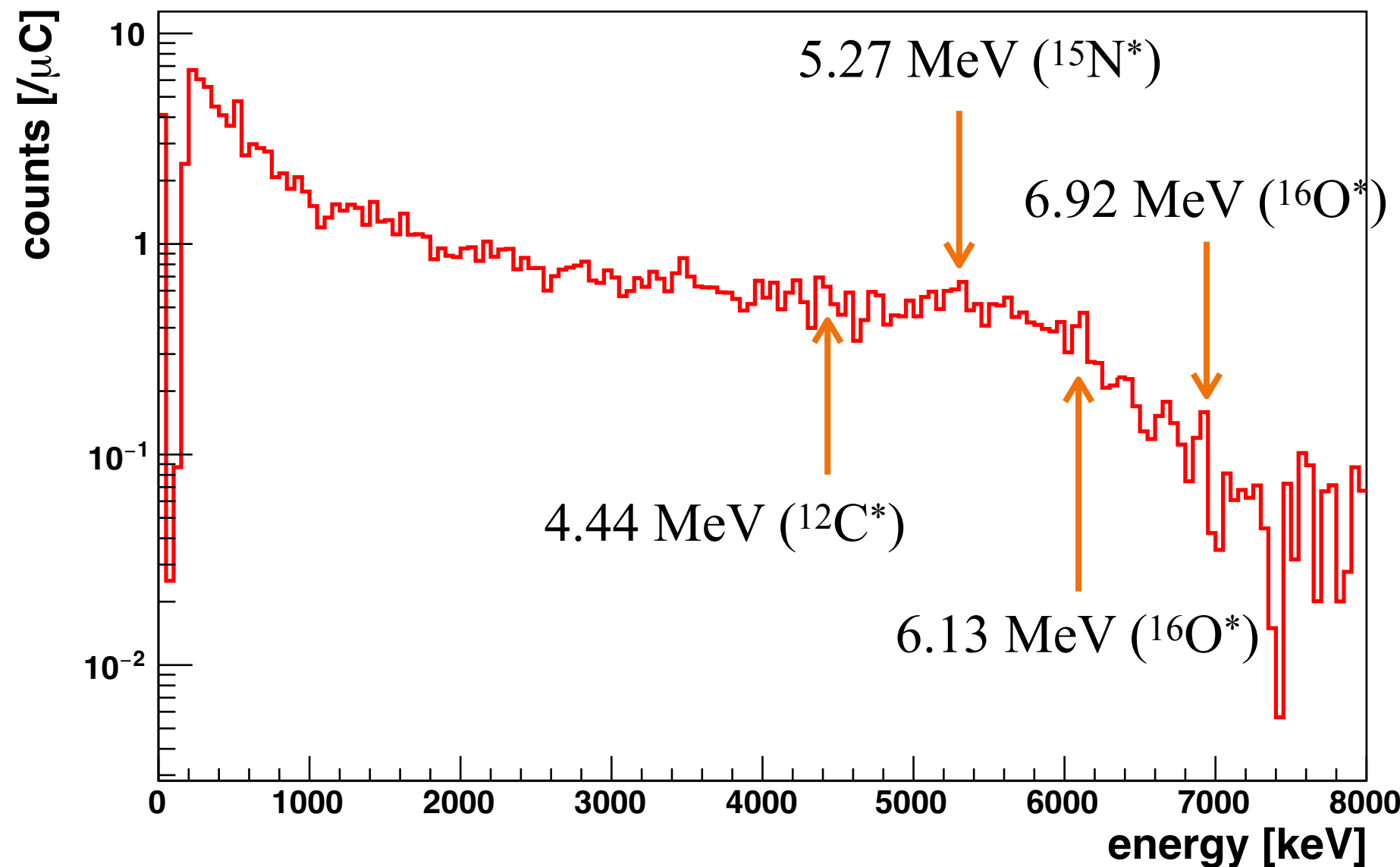
## Signal

$$\begin{aligned} \text{Signal} &= (\text{w/ water on} - \text{w/ water off}) \\ &\quad - (\text{w/o water on} - \text{w/o water off}) \end{aligned}$$



# Signal spectrum

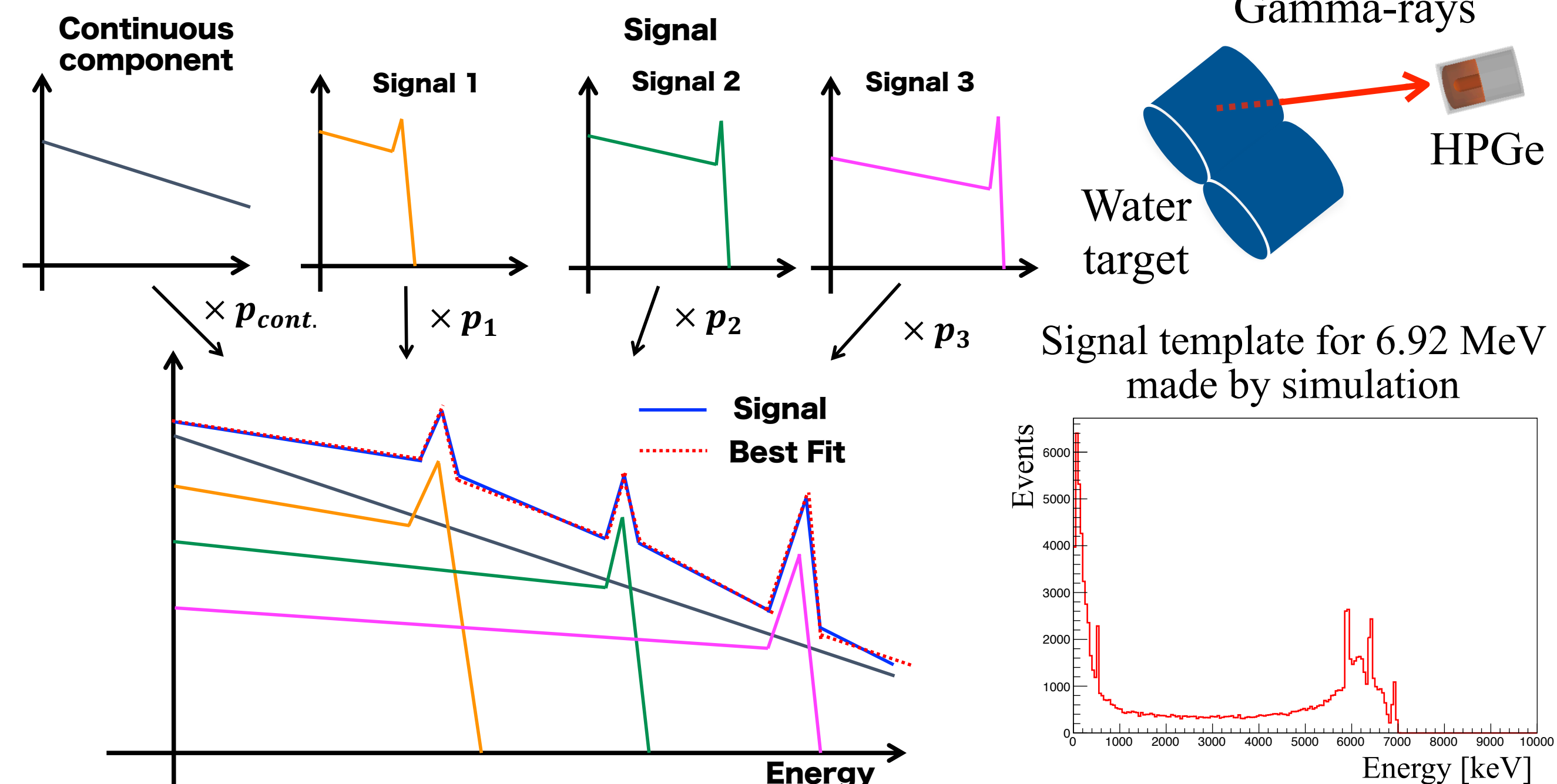
- $\gamma$ -rays emitted by the interaction of 235-270 MeV neutrons with  $^{16}\text{O}$
- This spectrum consists of  $\gamma$ -rays from  $^{16}\text{O}^*$ ,  $^{15}\text{N}^*$ ,  $^{12}\text{C}^*$  etc...
- Intensities of each  $\gamma$ -ray are extracted by spectrum fitting



# Spectrum fitting

15

- The signal spectrum is expressed as a linear combination of individual  $\gamma$ -rays and continuous component
- Relative intensity of each gamma-rays are extracted by fitting



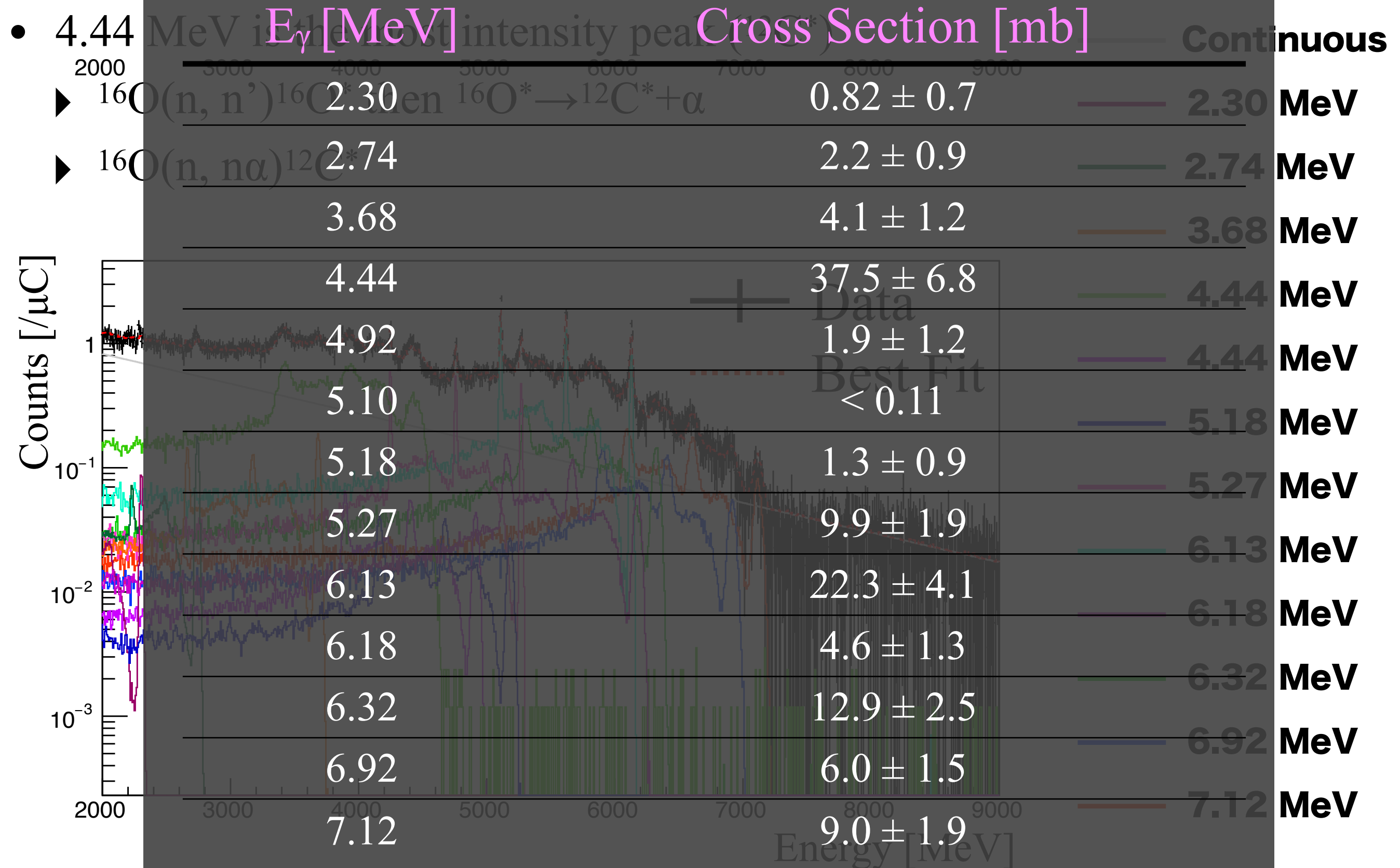
# Reaction

16

Energy [MeV]	Nucleus ( $J^\pi$ )	Process
2.30	$^{15}\text{N}(7/2^+)$	$^{16}\text{O}(\text{n}, \text{np})^{15}\text{N}^*$
2.74	$^{16}\text{O}(2^-)$	$^{16}\text{O}(\text{n}, \text{n}')^{16}\text{O}^*$
3.68	$^{13}\text{C}(3/2^-)$	$^{16}\text{O}(\text{n}, \alpha)^{13}\text{C}^*$
4.44	$^{12}\text{C}(2^+)$	$^{16}\text{O}(\text{n}, \text{n}\alpha)^{12}\text{C}^*$ etc ...
4.91	$^{14}\text{N}(0^-)$	$^{16}\text{O}(\text{n}, 2\text{np})^{14}\text{N}^*$
5.10	$^{14}\text{N}(2^-)$	$^{16}\text{O}(\text{n}, 2\text{np})^{14}\text{N}^*$
5.18	$^{15}\text{O}(1/2^+)$	$^{16}\text{O}(\text{n}, 2\text{n})^{15}\text{O}^*$ etc ...
5.27	$^{15}\text{N}(5/2^+)$	$^{16}\text{O}(\text{n}, \text{np})^{15}\text{N}^*$ etc ...
6.13	$^{16}\text{O}(3^-)$	$^{16}\text{O}(\text{n}, \text{n}')^{16}\text{O}^*$
6.18	$^{15}\text{O}(3/2^-)$	$^{16}\text{O}(\text{n}, 2\text{n})^{15}\text{O}^*$ etc ...
6.32	$^{15}\text{N}(3/2^-)$	$^{16}\text{O}(\text{n}, \text{n}'\text{p})^{15}\text{N}^*$
6.92	$^{16}\text{O}(2^+)$	$^{16}\text{O}(\text{n}, \text{n}')^{16}\text{O}^*$
7.12	$^{16}\text{O}(1^-)$	$^{16}\text{O}(\text{n}, \text{n}')^{16}\text{O}^*$

# Fitting results (30 MeV)

## Cross Section



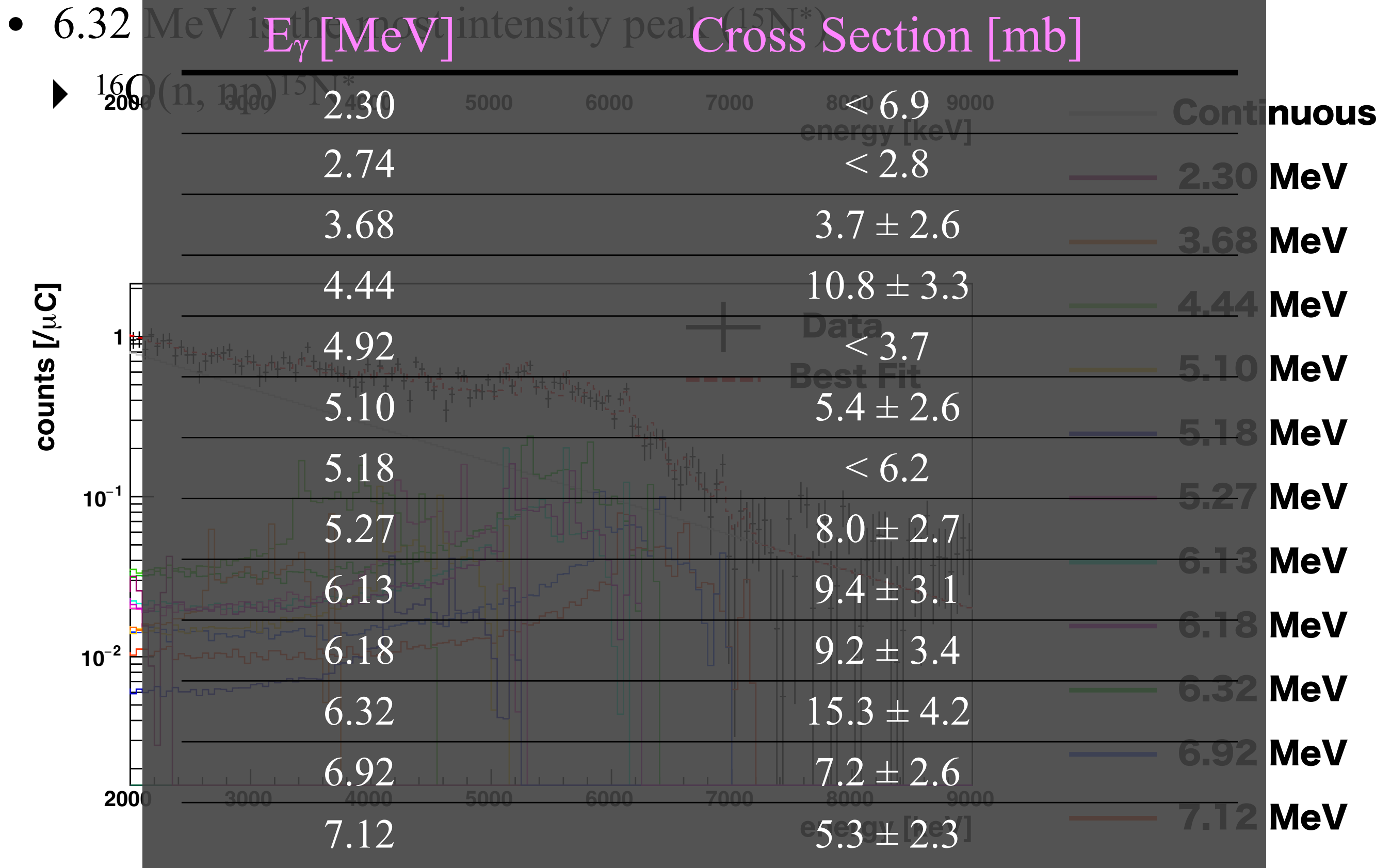
# Fitting results (80 MeV) Cross Section

- 6.32 MeV is the post intensity peak  $E_\gamma$  [MeV]
- $^{16}\text{O}(n, np)^{15}\text{N}^*$



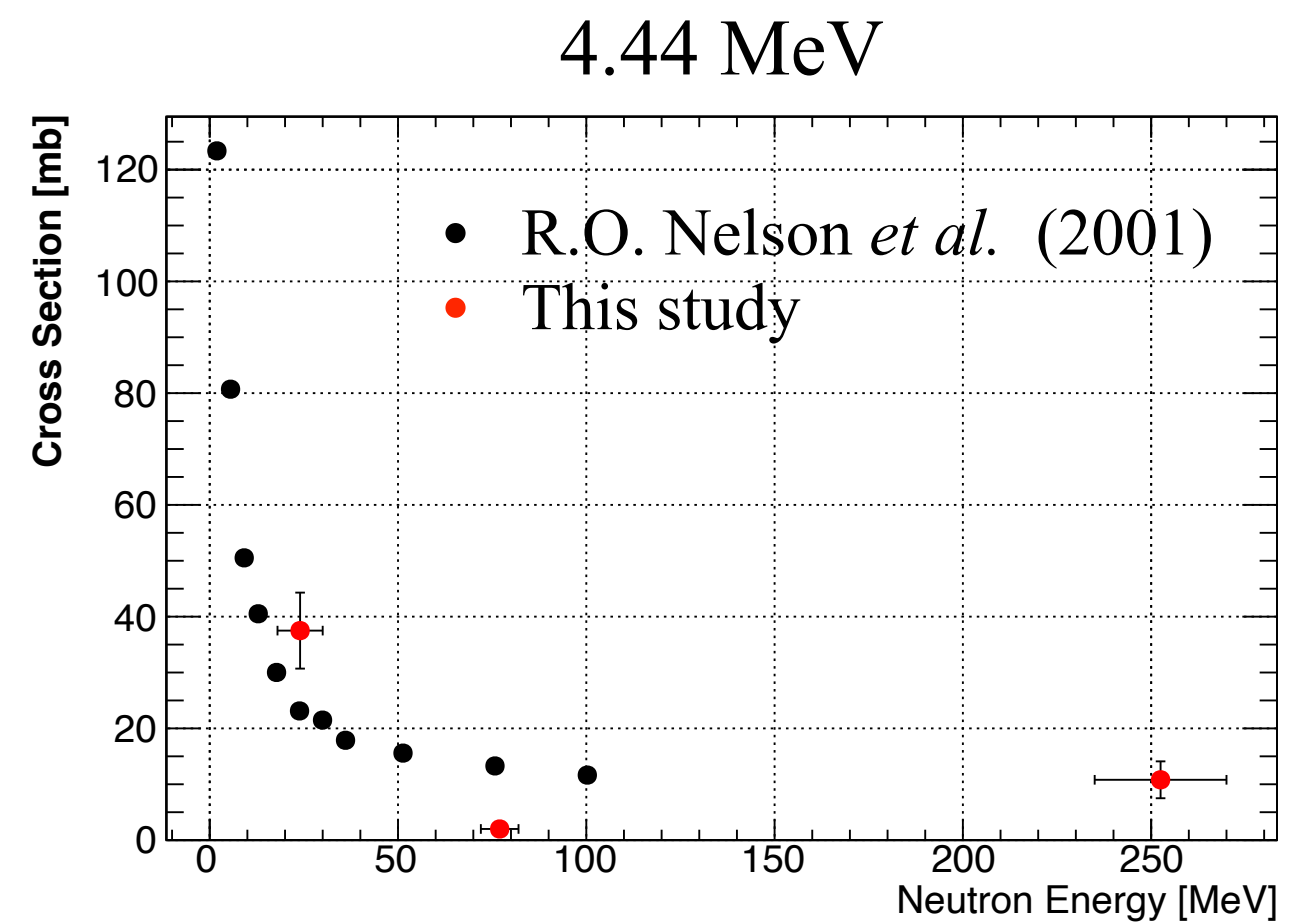
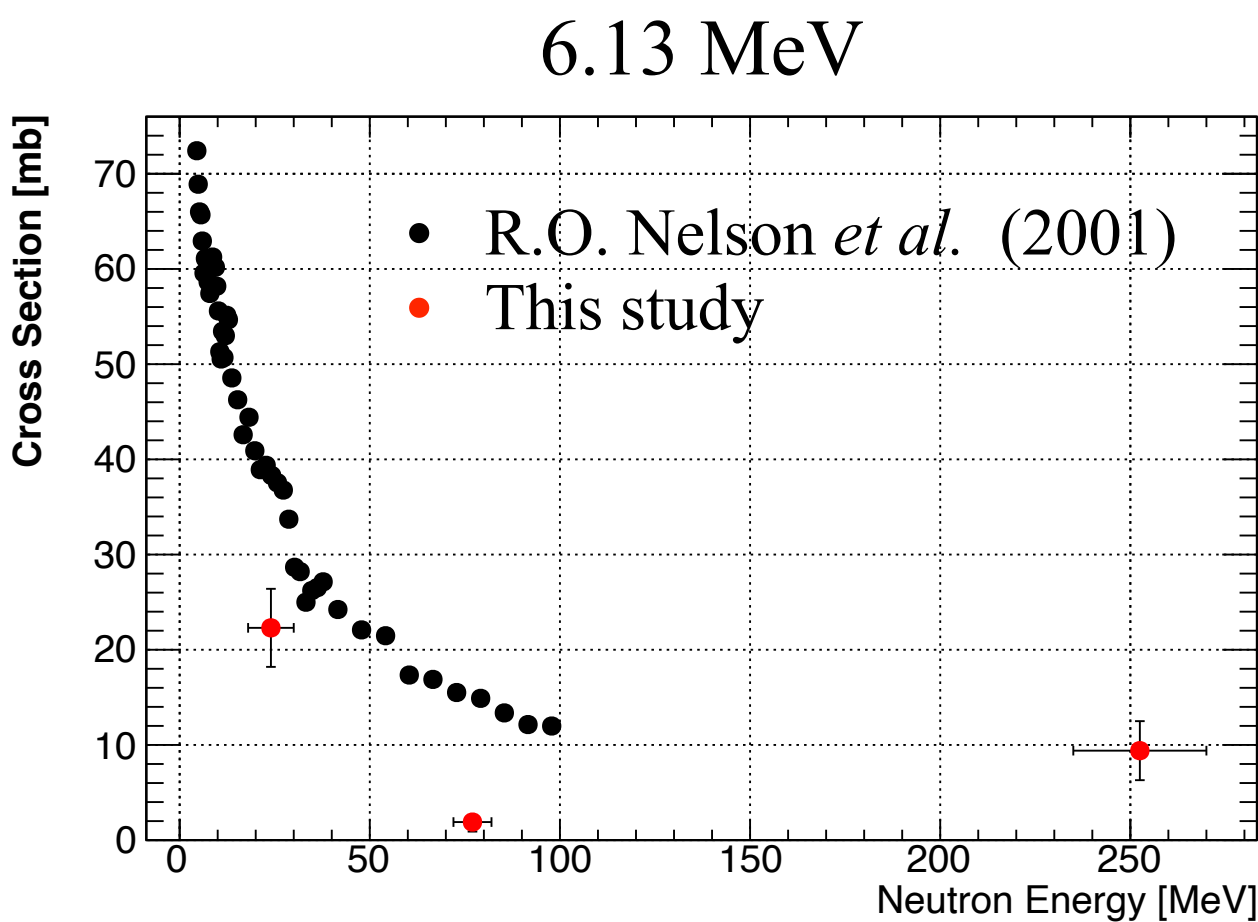
# Fitting results (250 MeV)

## Cross Section



# Comparison with previous study

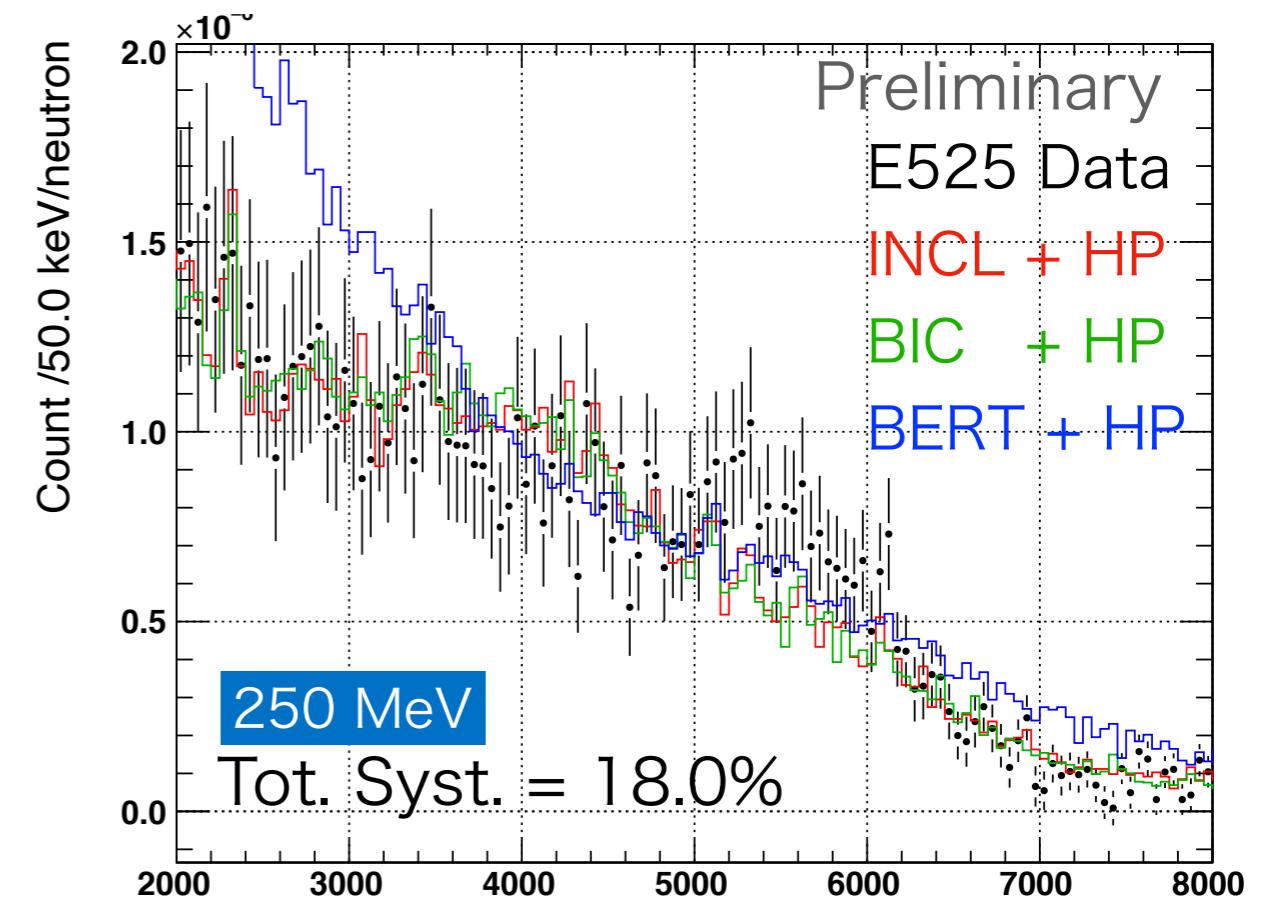
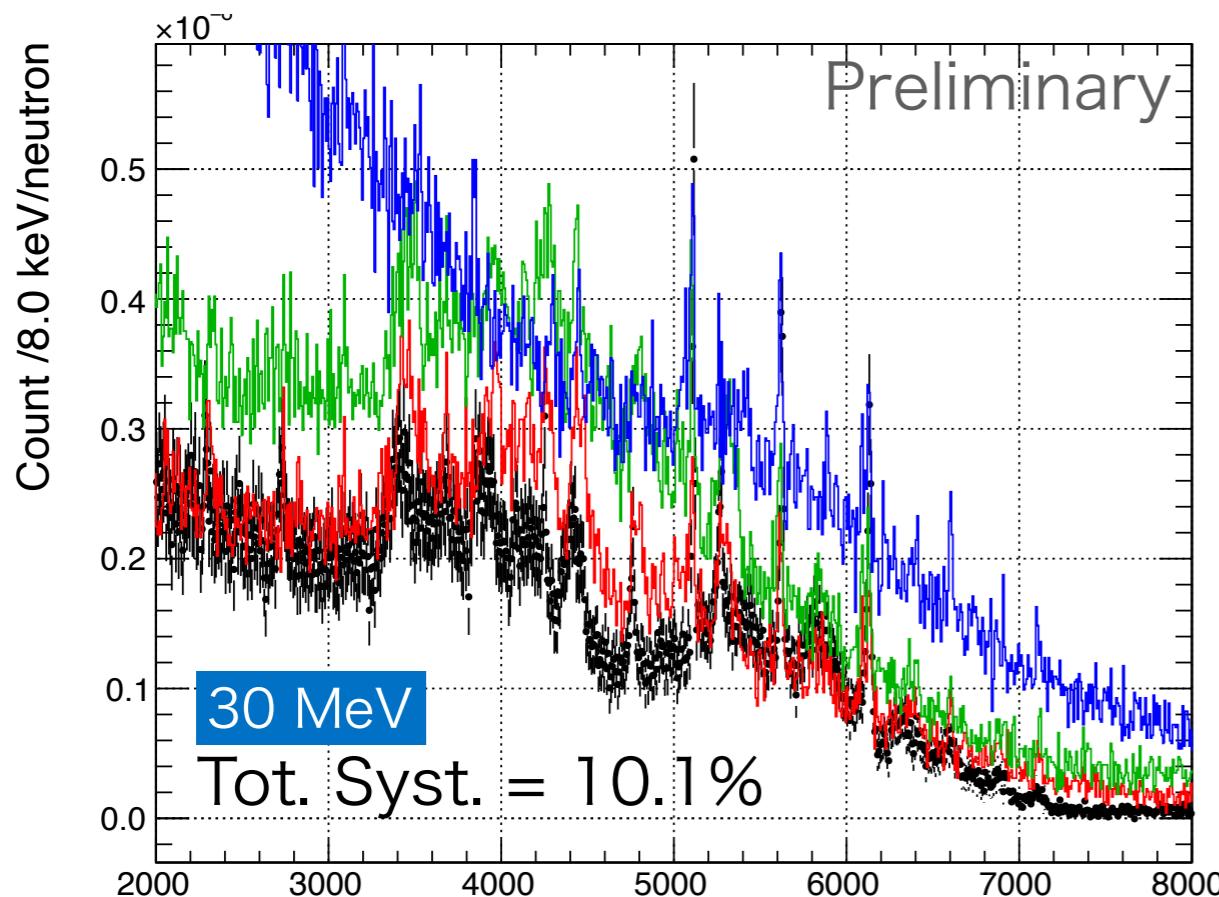
- The result of E525 (30, 250 MeV) is roughly consistent with R.O. Nelson et al. (2001).
- E487 (80 MeV) shows smaller cross section result than the other results.
  - Non-linearity of proton current measurement cause the underestimation for cross section



R.O. Nelson et al., Nucl. Sci. Eng. 138, 105 (2001)

# Comparison with simulation models

- INCL++ and BIC show better agreements with observed data in 30 MeV and 250 MeV
- Reported by Hino-san in the poster session



Model	$\chi^2/\text{ndf} @ 30 \text{ MeV}$	$\chi^2/\text{ndf} @ 250 \text{ MeV}$
INCL++	1933.4 / 750	122.4 / 120
BIC	2405.5 / 750	133.0 / 120
BERT	4632.9 / 750	238.6 / 120

# Summary

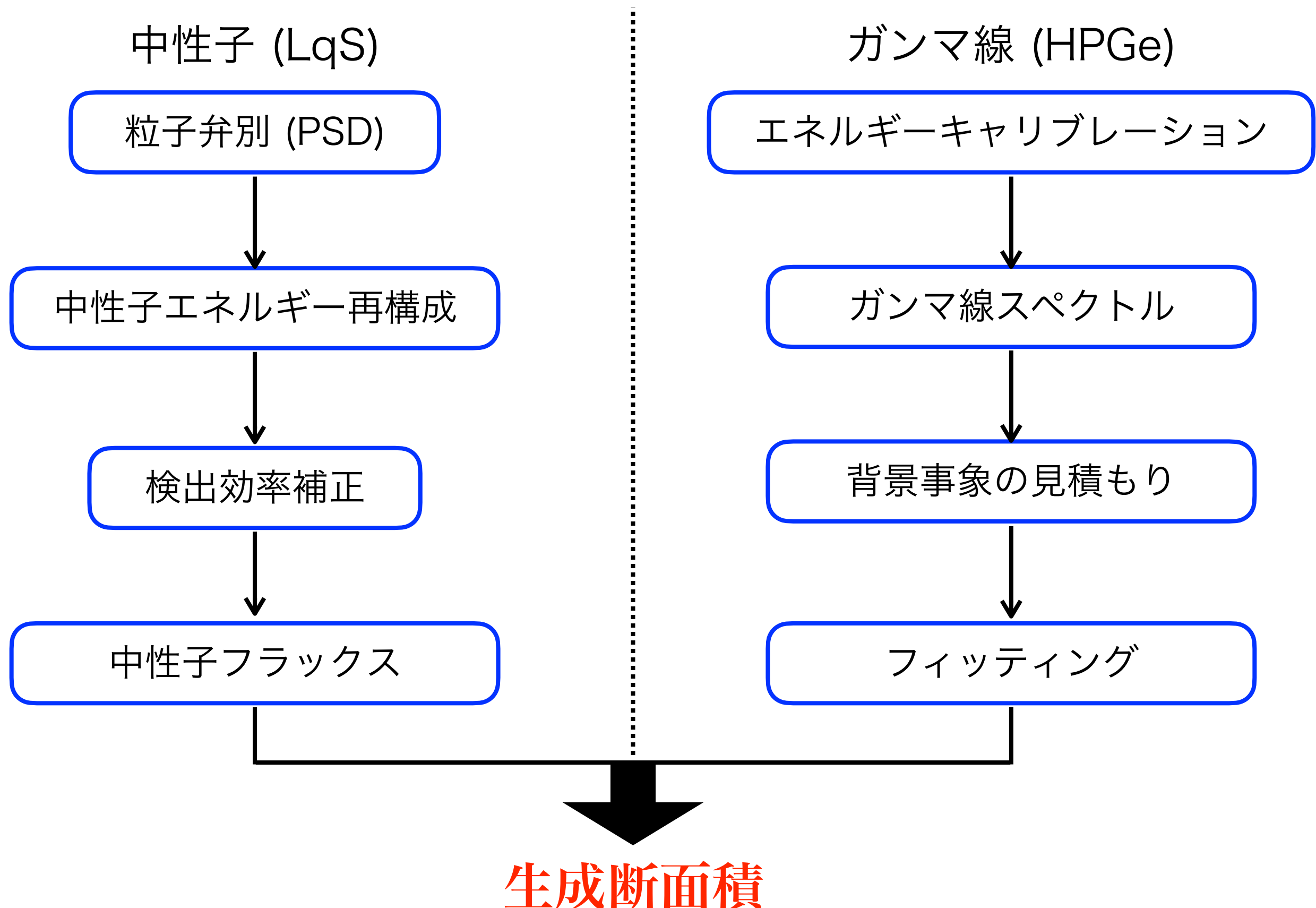
22

- It is important for SRN search to understand neutron- $^{16}\text{O}$  interaction
- We measured  $\gamma$ -rays produced from neutron- $^{16}\text{O}$  reaction using 30, 80 and 250 MeV neutron
- Data analysis
  - Neutron flux was estimated after particle identification and energy reconstruction
  - Relative intensity was obtained by spectrum fitting
  - Cross sections for each  $\gamma$ -rays were calculated
- Comparison with nucleon-nuclear interaction model was reported by Hino-san
  - INCL++ and BIC have the better agreement in both 30 and 250 MeV

# Backup

# 解析の流れ

24



# 粒子弁別 (LqS)

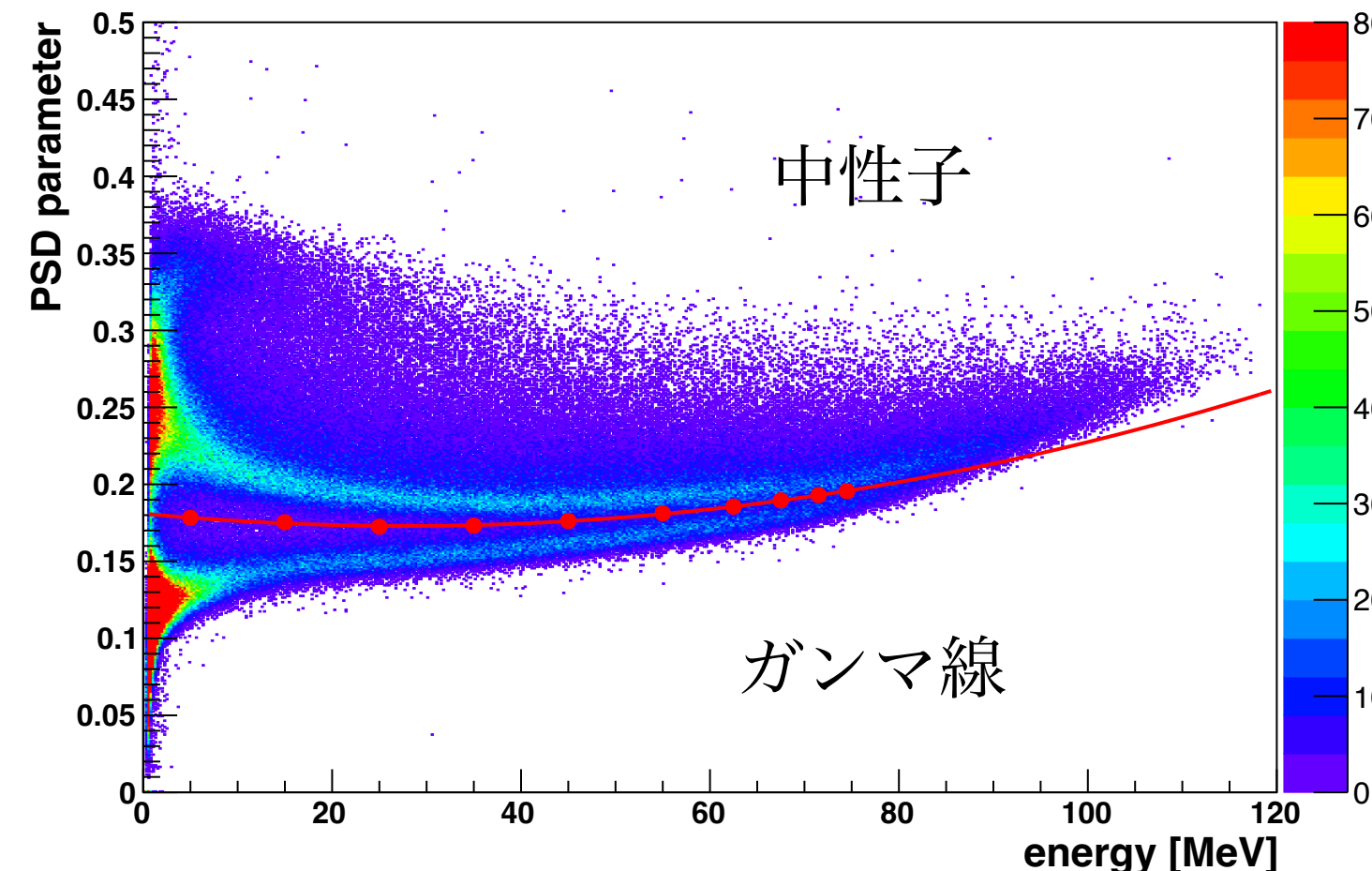
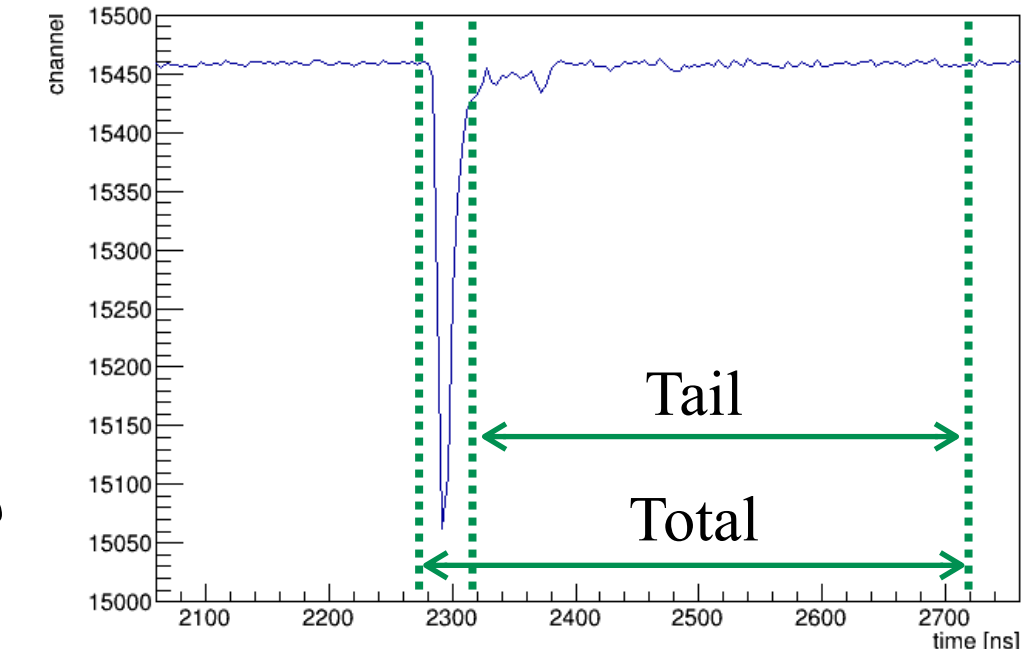
25

- 波形の違いを利用して中性子イベントを選別

( Pulse Shape Discrimination )

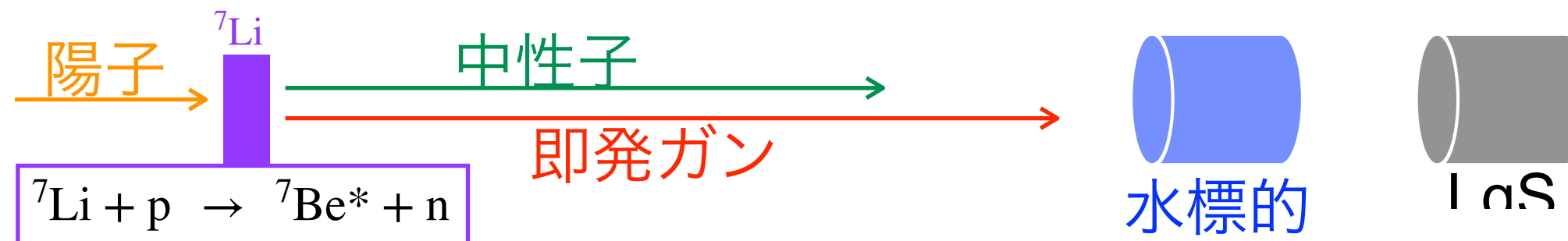
$$\text{PSD parameter} = \frac{\text{Tail}}{\text{Total}}$$

- 中性子イベントはテールが長くなる  
→ PSD parameter が大きい

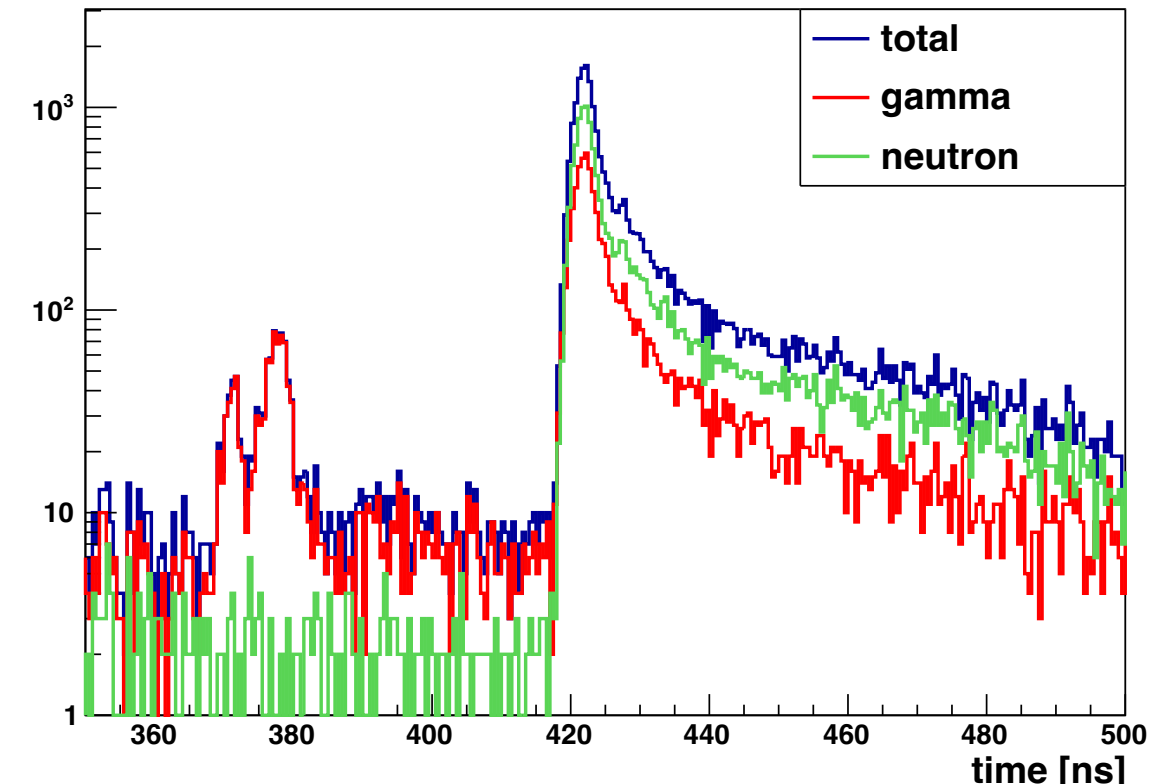


- エネルギー領域毎に中性子と  
ガンマ線のカット条件を決定

# エネルギー再構成 (LqS)



- 即発ガンマ線 :  $\text{Be}^*$  の脱励起ガンマ線
- $\text{LqS}$ まで光速で飛来する  
→ 中性子と飛来時間差  $\Delta t$  が生じる
- ToF分布を作成  
→ 即発ガンマ線のピークと  
中性子のピークを確認
- 下の式を用いてエネルギー再構成



$$K = \frac{mc^2}{\sqrt{1 - \left(\frac{1}{1 + \frac{c}{L}}\Delta t\right)^2}} - mc^2$$

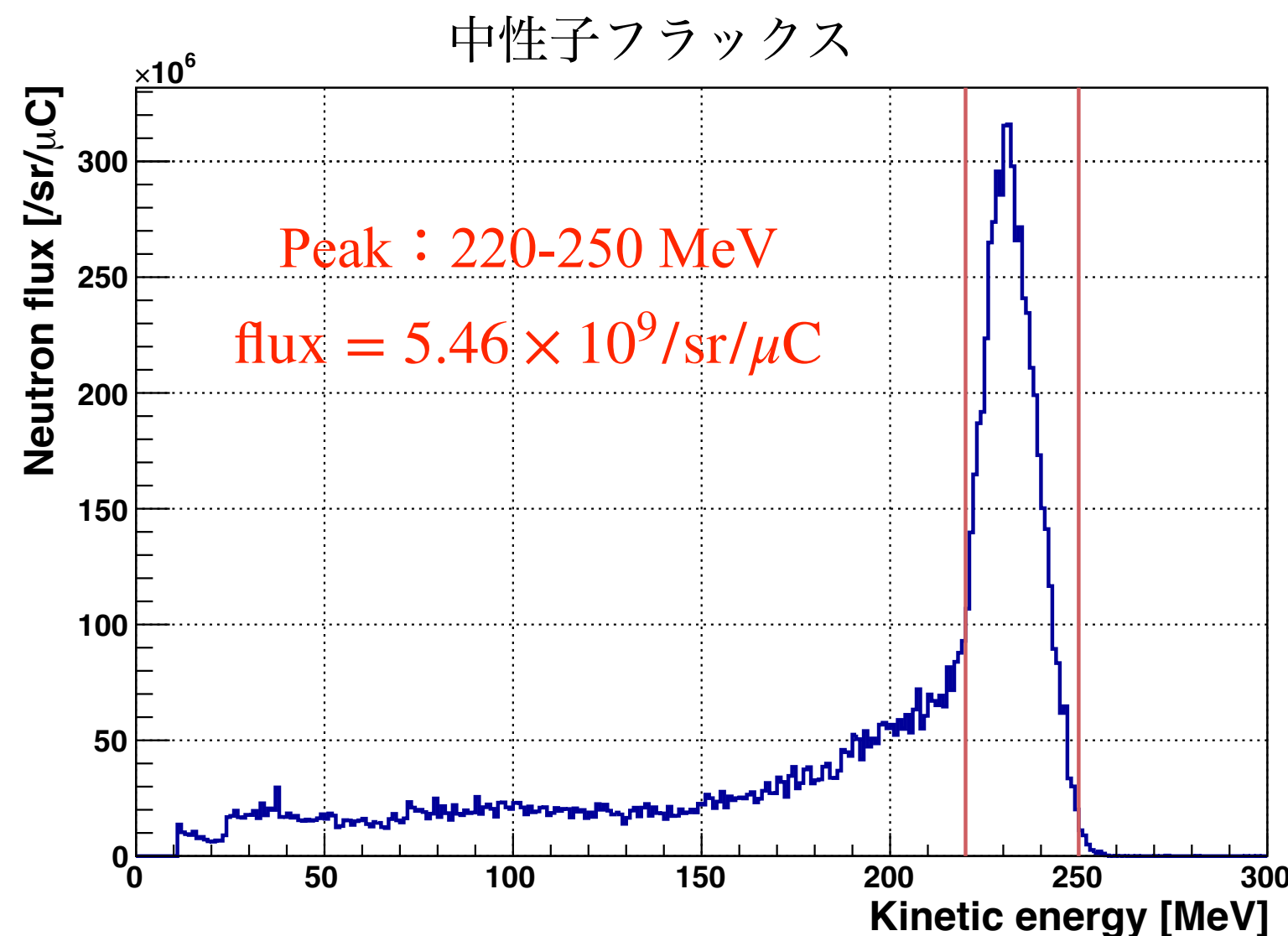
$mc^2$  : 中性子の質量 (939.6 MeV)

$L$  : Liターゲットから水標的までの距離

$\Delta t$  : 飛来時間の差

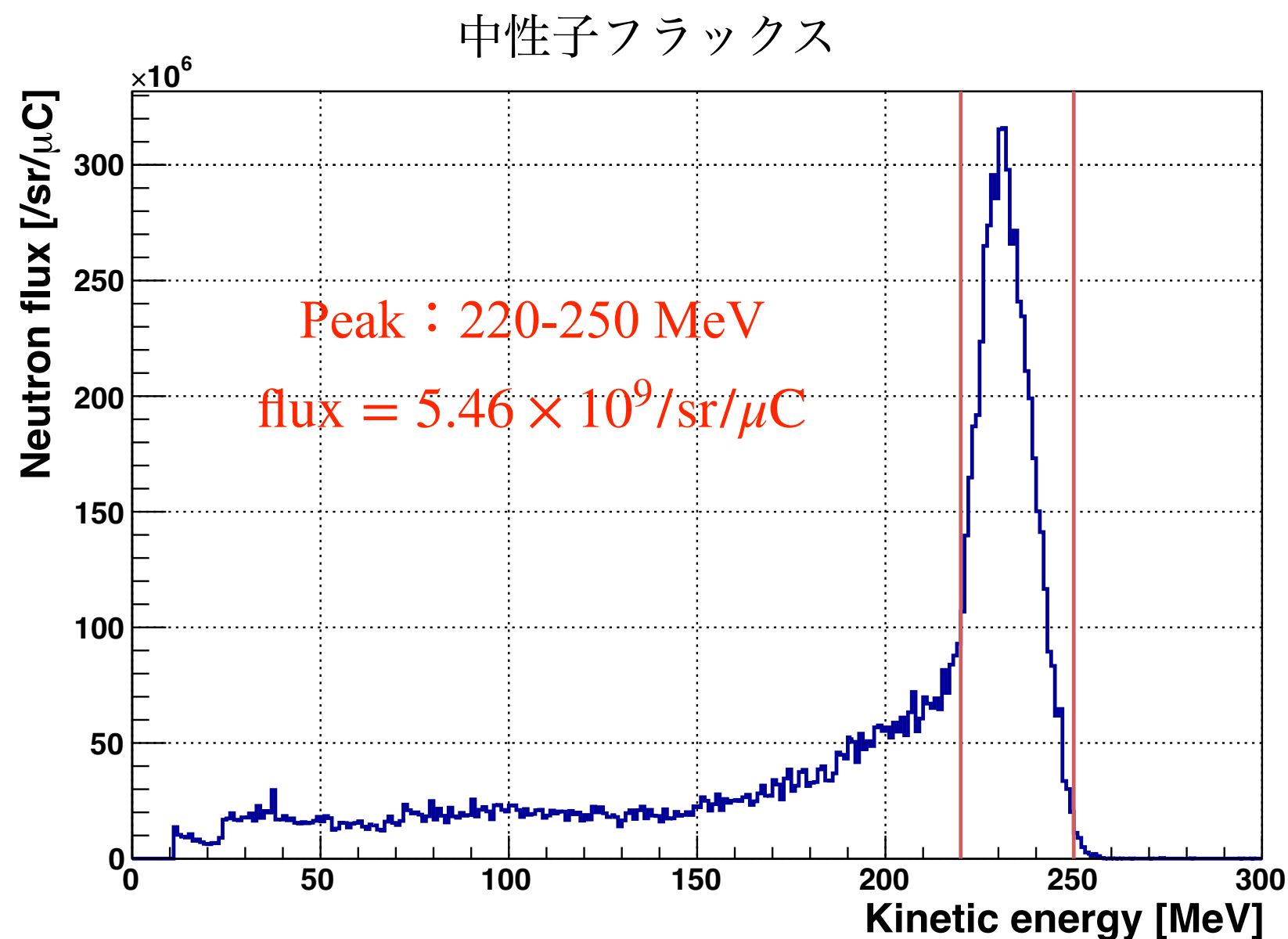
# 中性子フラックス (LqS)

- シミュレーションを用いて LqS の中性子検出効率を計算
- 中性子フラックスを算出
- ピーク領域は 220 - 250 MeV  
→ この領域の中性子を断面積計算に用いる



# 中性子flux

- 中性子fluxを算出
- ピーク領域は220 - 250 MeV  
→ この領域の中性子を断面積計算に用いる

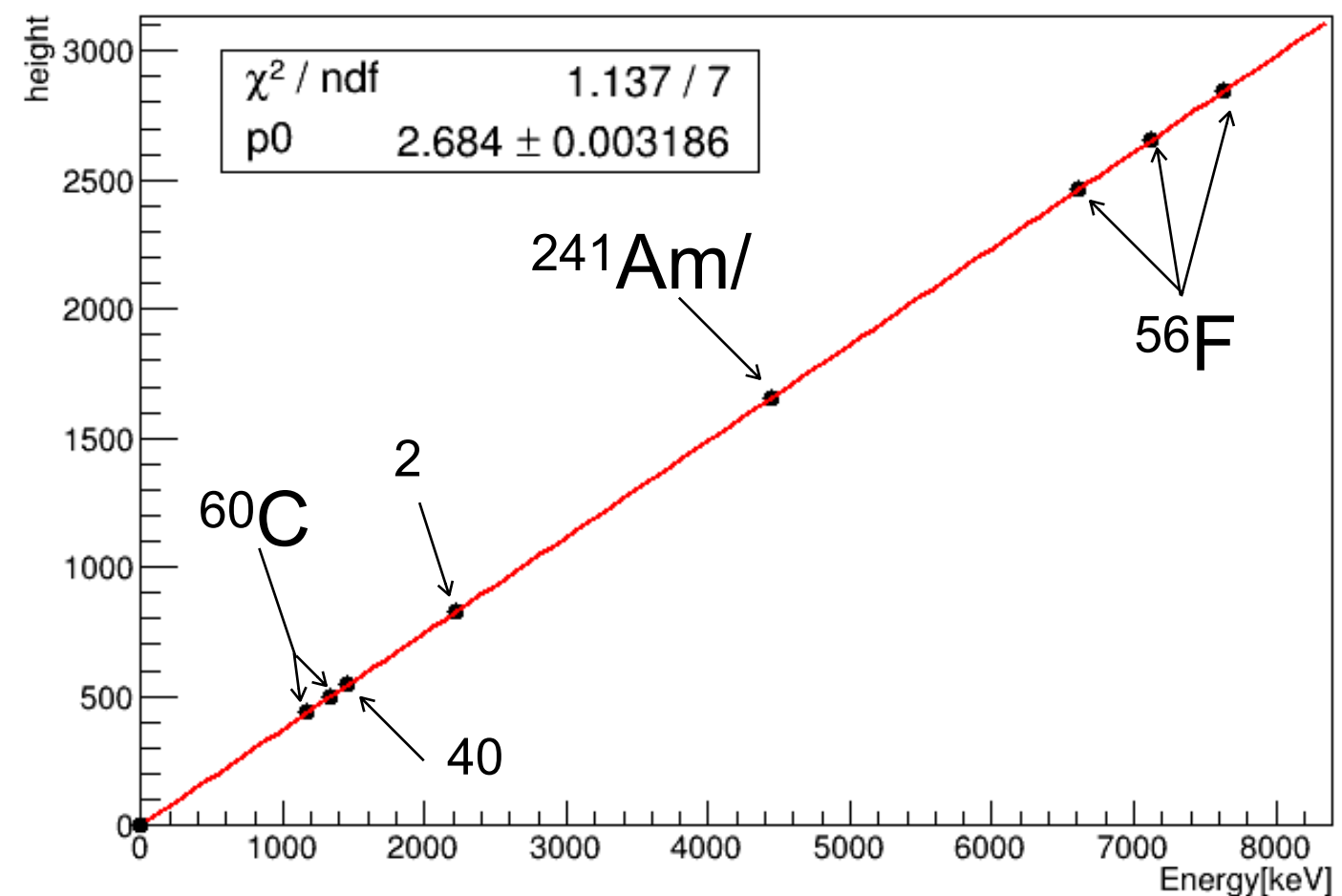


# エネルギーキャリブレーション(Ge)

29

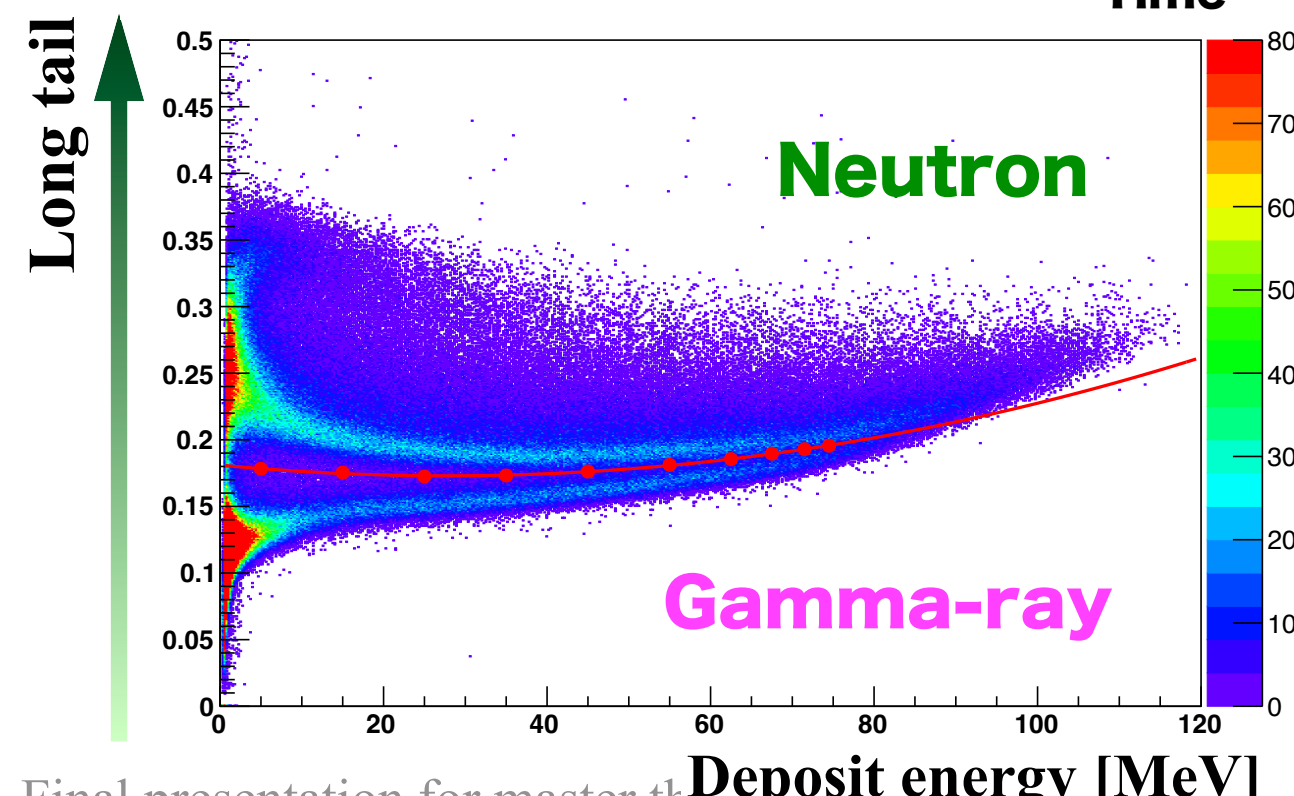
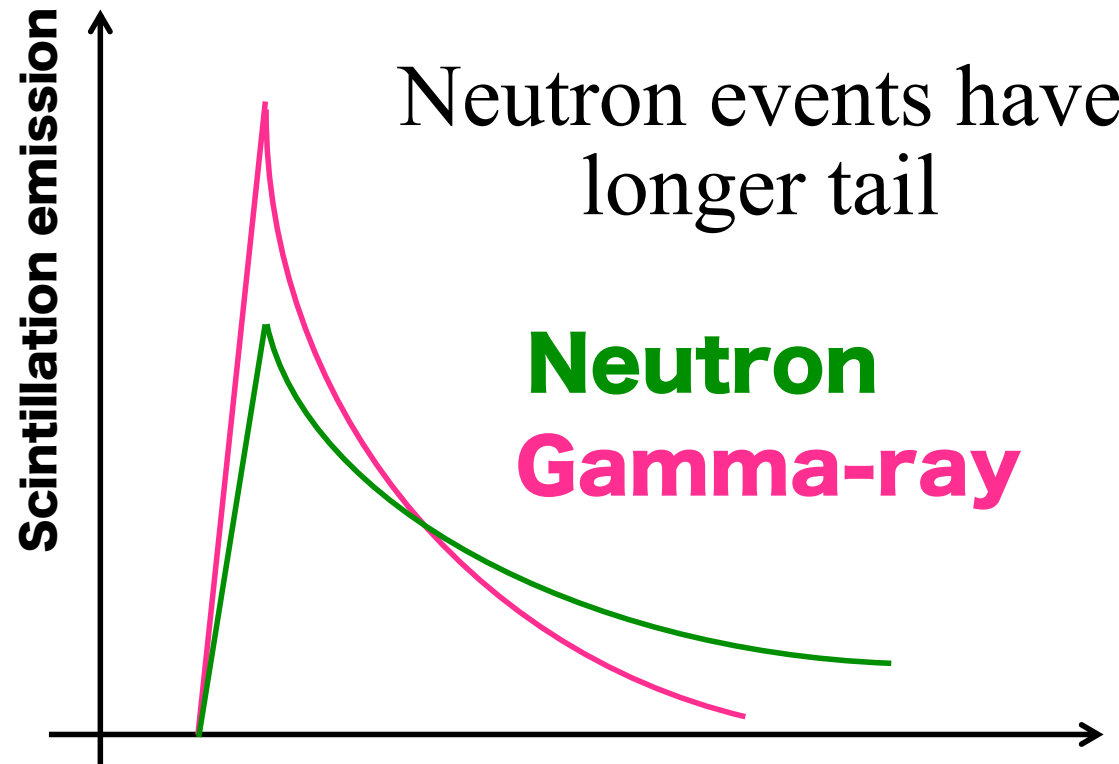
$^{60}\text{Co}$	1.17 MeV, 1.33 MeV
$^{241}\text{Am}/\text{Be}$	4.44 MeV
$^{56}\text{Fe}$	7.63 MeV + S.E. + D.E.
$^{40}\text{K}$ (環境)	1.46 MeV
$^1\text{H}$ (熱中性子捕獲)	2.22 MeV

- 上記のガンマ線を用いて HPGe検出器のエネルギー キャリブレーションを行なった
- 信号が予想される6 MeV付近を 含め、良い線形性を確認

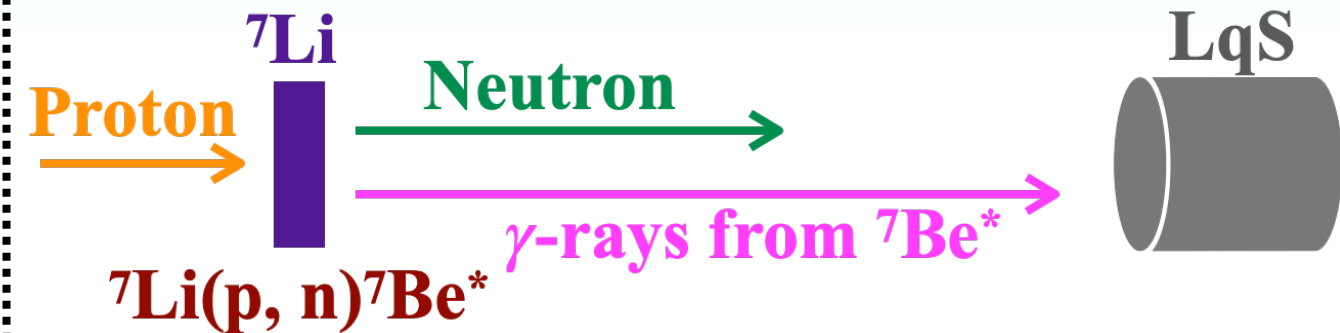


# Event selection and reconstruction

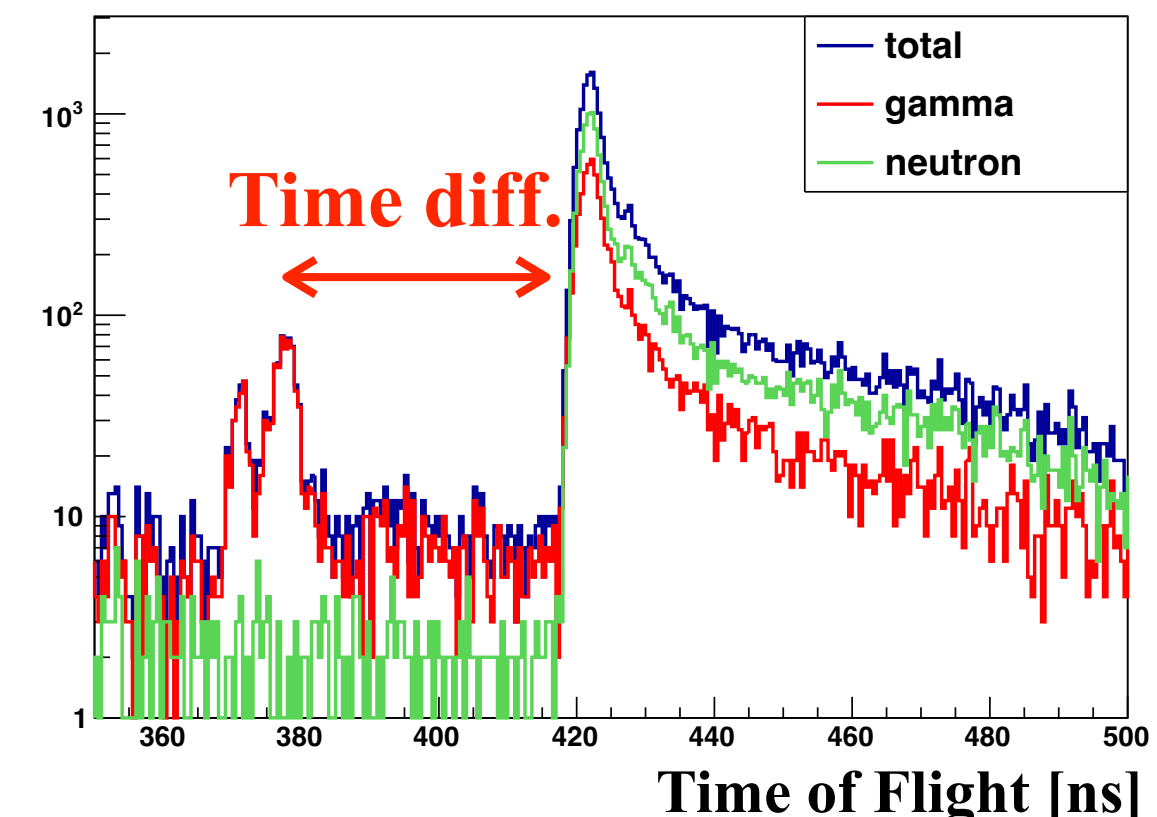
## Event cut for neutron selection



## Kinetic energy reconstruction

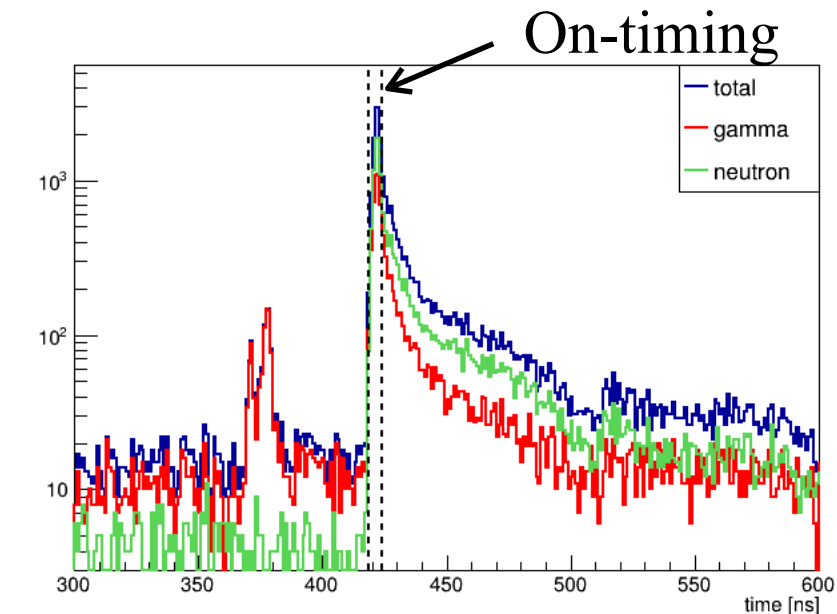


- $\gamma$ -rays from  ${}^7\text{Be}^*$  enter the LqS before neutrons
- Energies of neutrons are calculated based on the time difference



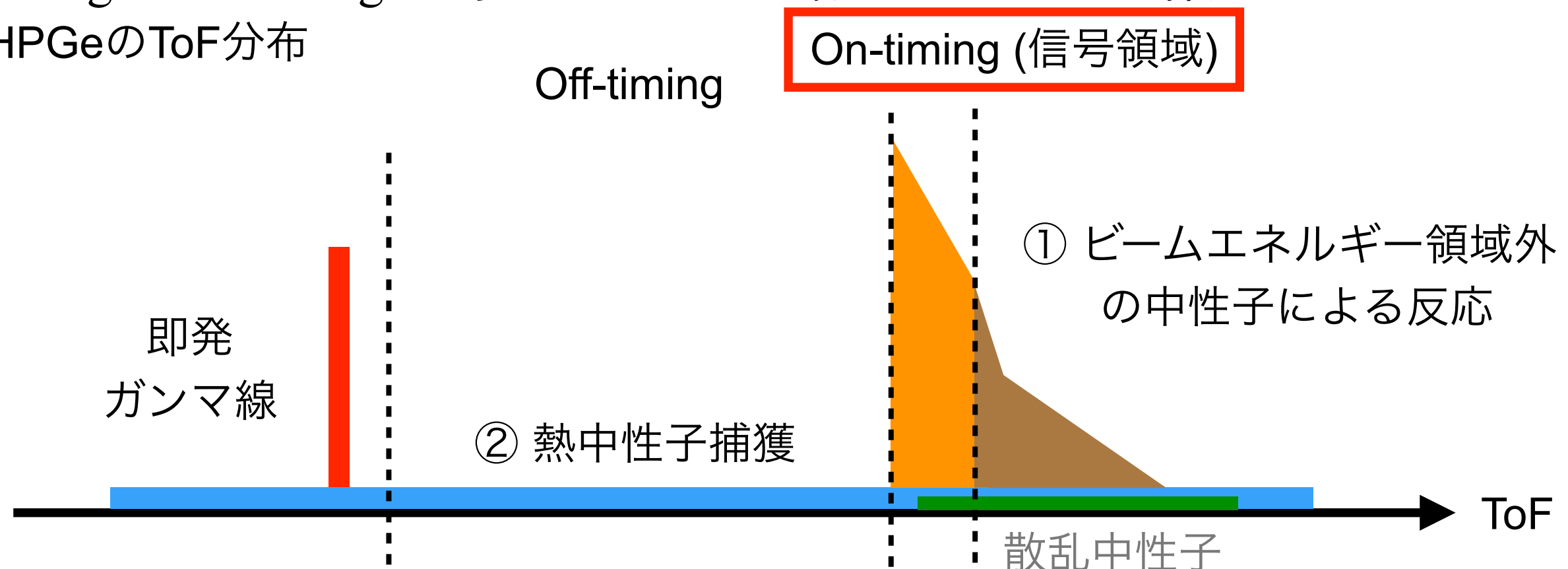
# 背景事象の見積もり

- 信号事象：220-250 MeV の中性子と水の反応によるガンマ線
- 主な背景事象
  - ① ビームエネルギー領域外の中性子による反応  
→ ToFを用いたカット
  - ② 熱中性子捕獲  
→ Off-timing 領域のイベントを用いる



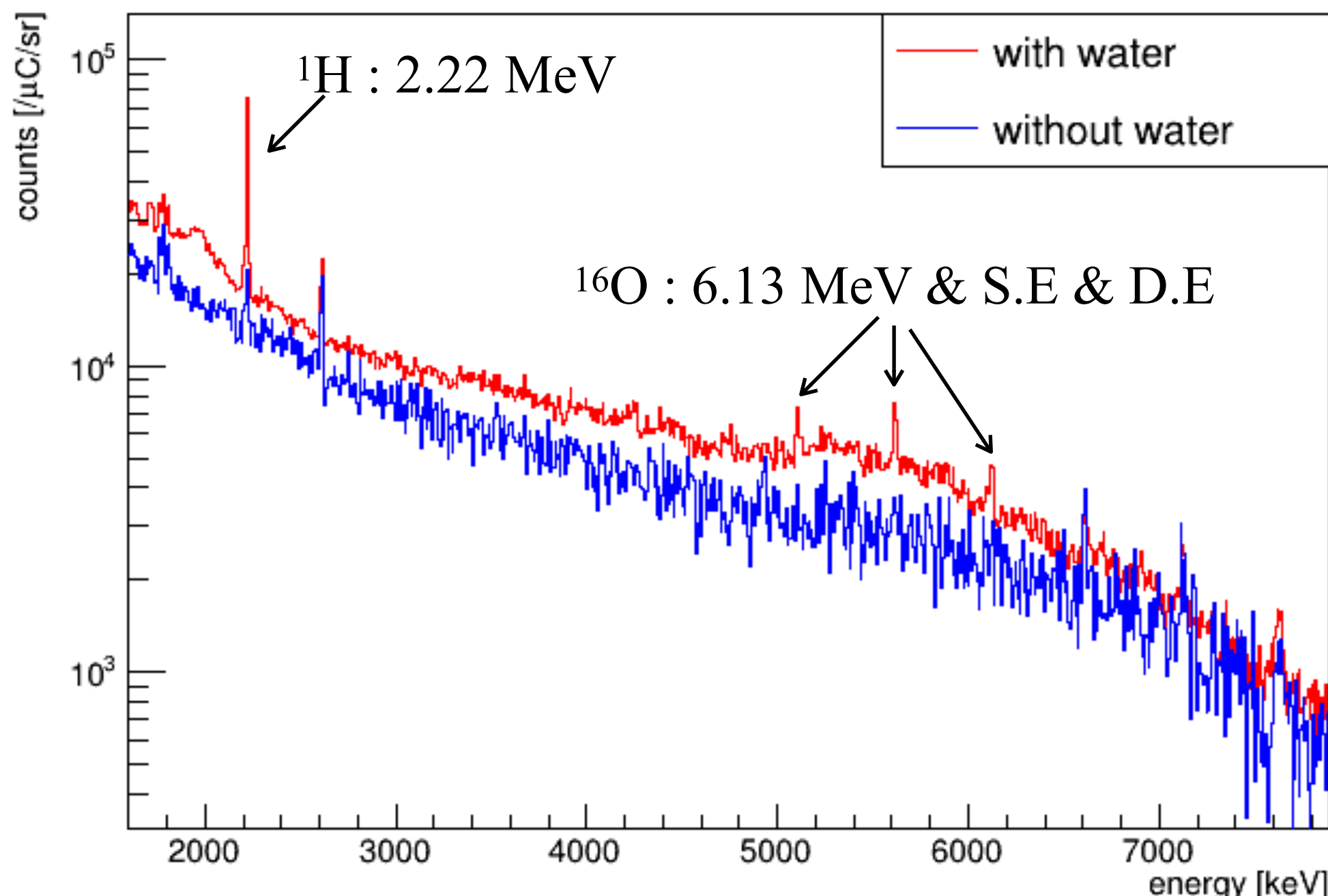
On-timing・Off-timing を考慮したガンマ線スペクトルを作成

HPGeのToF分布



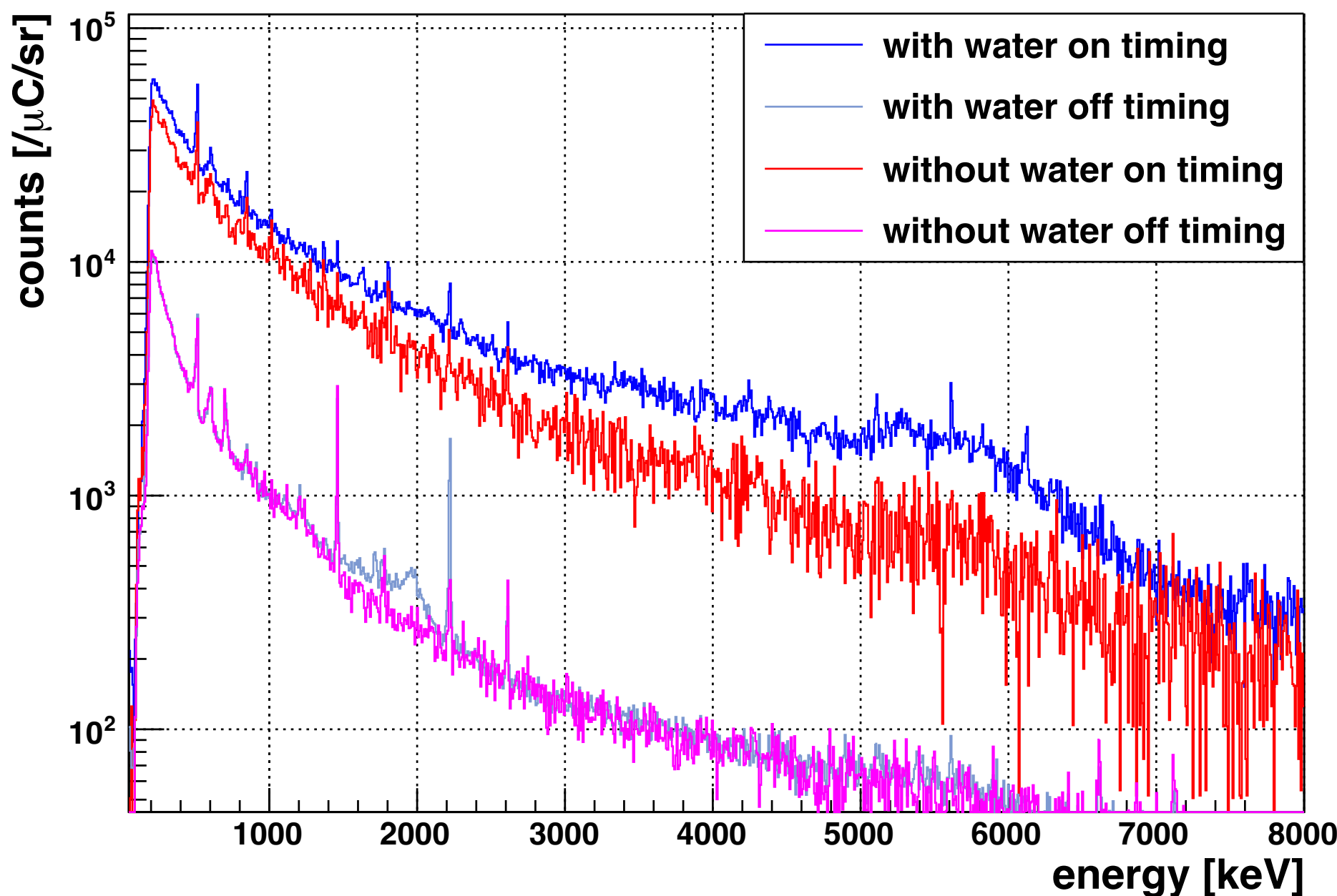
# ガンマ線スペクトル

- 以下のようなガンマ線スペクトルが得られた
- $^1\text{H}$ の熱中性子捕獲や $^{16}\text{O}$ 由来のものなど、複数のピークが見られる
- このスペクトルから背景事象を差し引く



# Timing 別のスペクトル

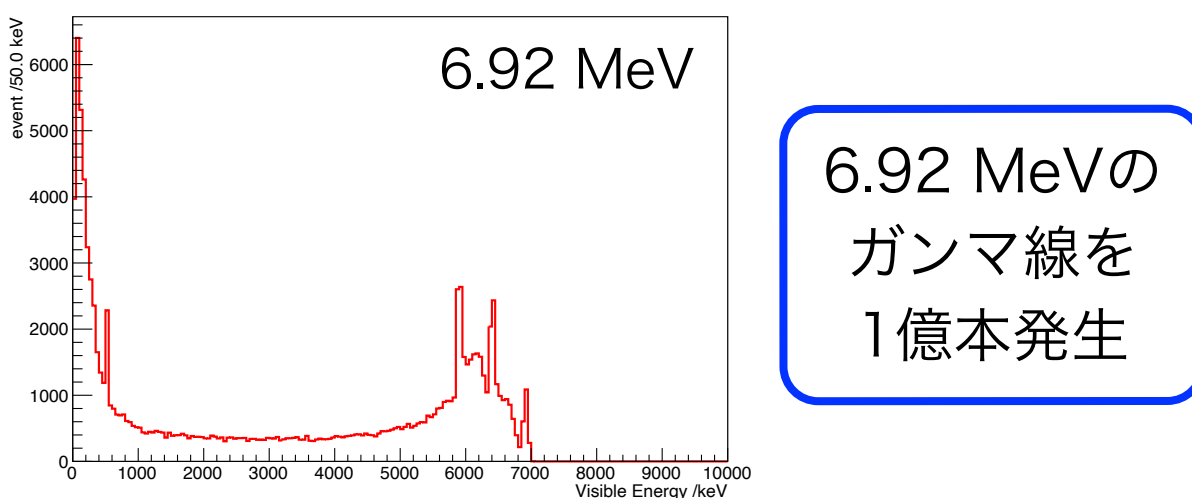
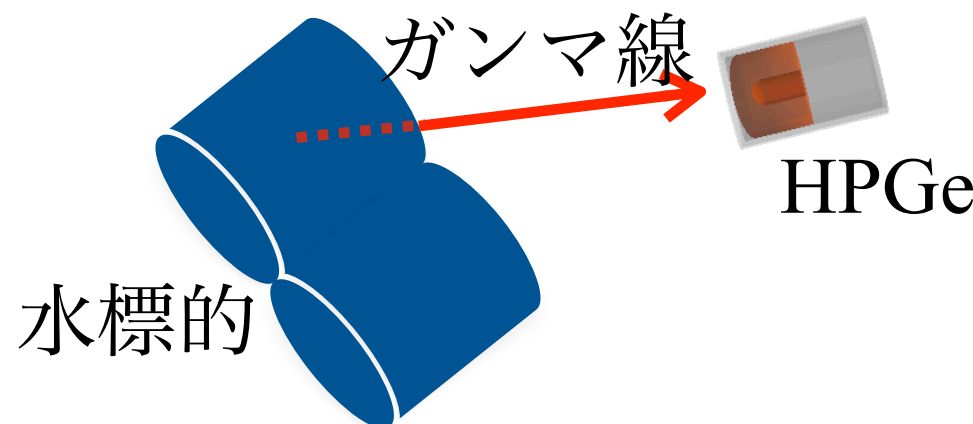
- w/ water ( on / off timing )、w/o water ( on / off timing )の計4つのスペクトル図を作成
- これらの分布を利用して背景事象を差し引く



# スペクトルフィッティング

- ・ フィッティングを行い、各ガンマ線の生成断面積を求める

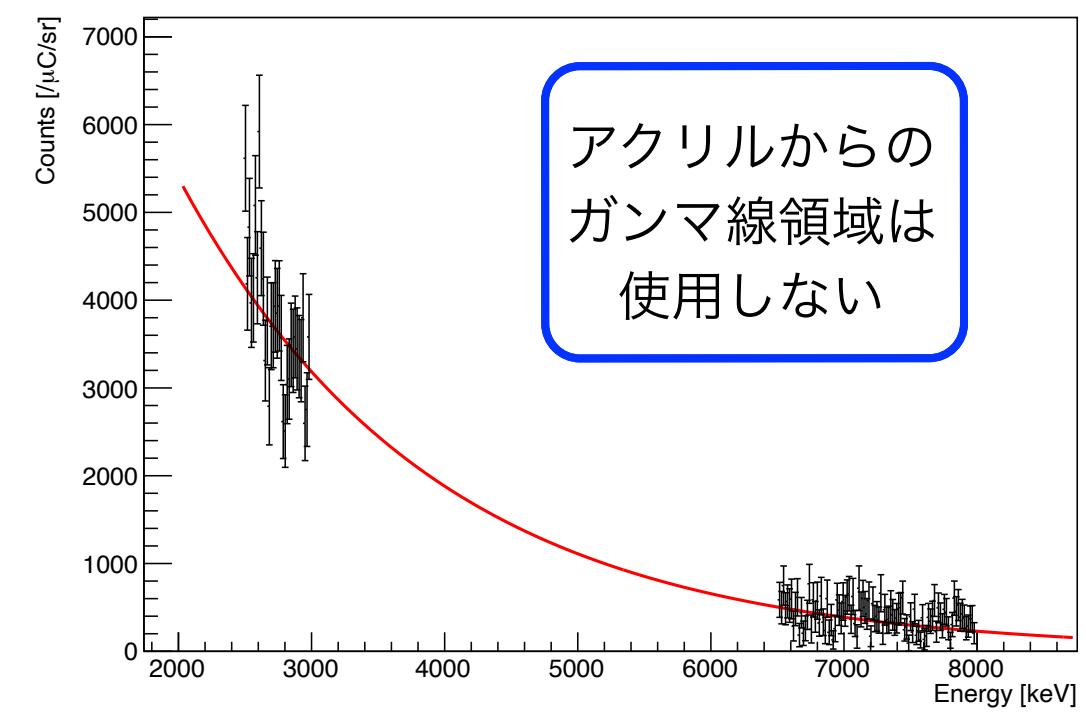
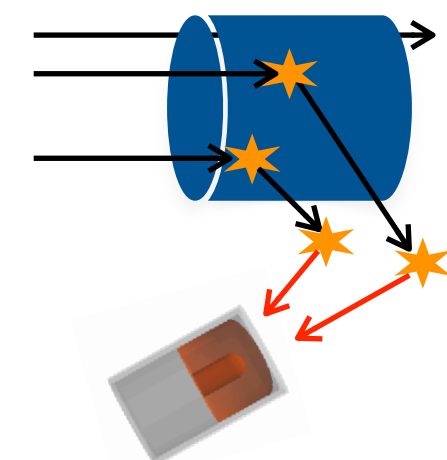
Signal template



計10個のガンマ線について  
同様にテンプレートを作成

Background template

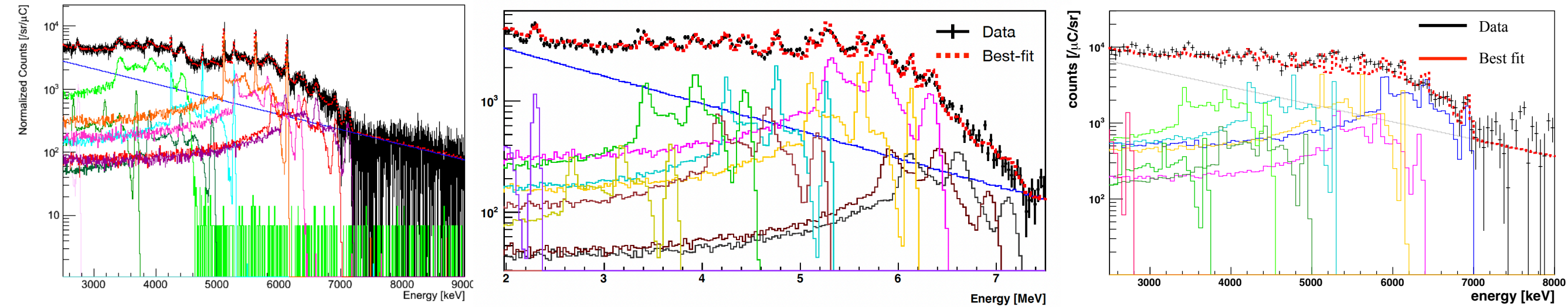
- ・ 水標的で散乱された中性子が周辺の物質と反応して生じるガンマ線
- ・ 水なしランを用いて作成
- ・ 指数関数を仮定



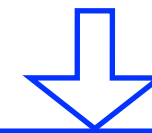
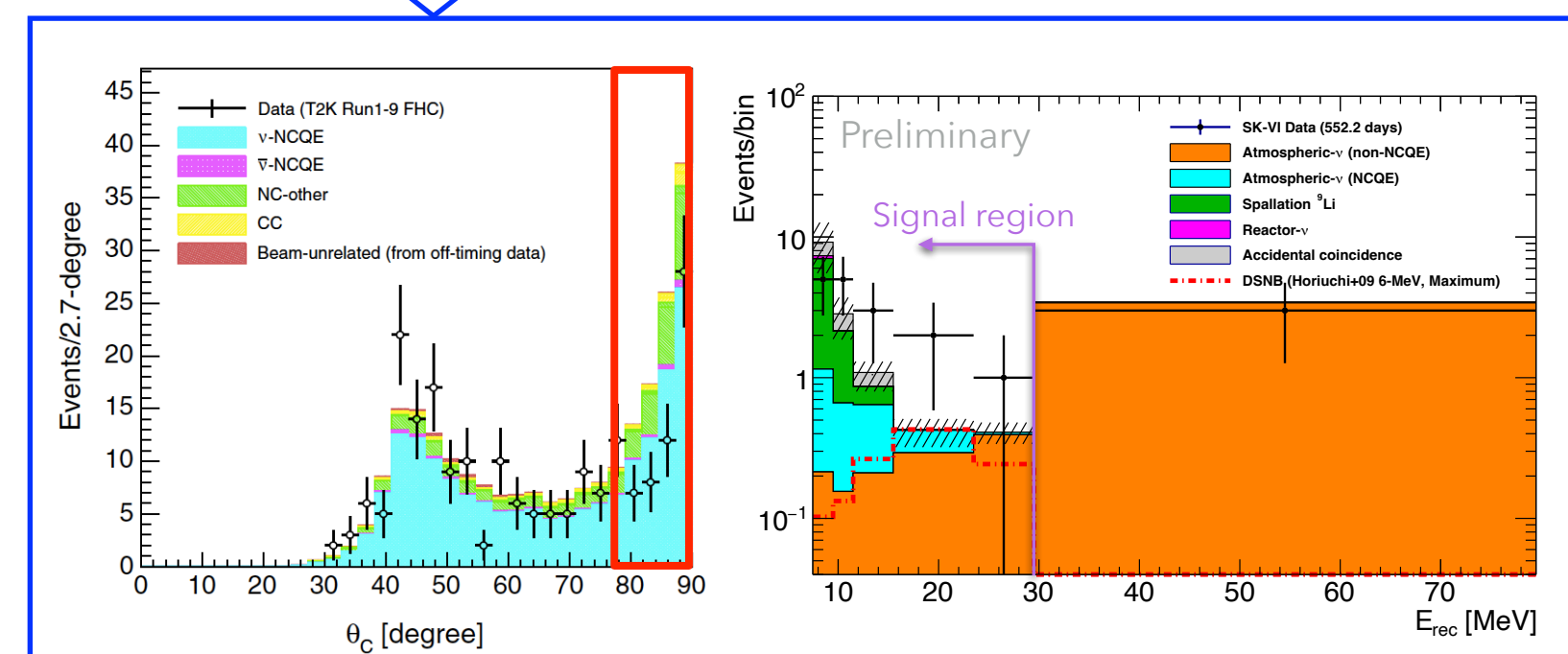
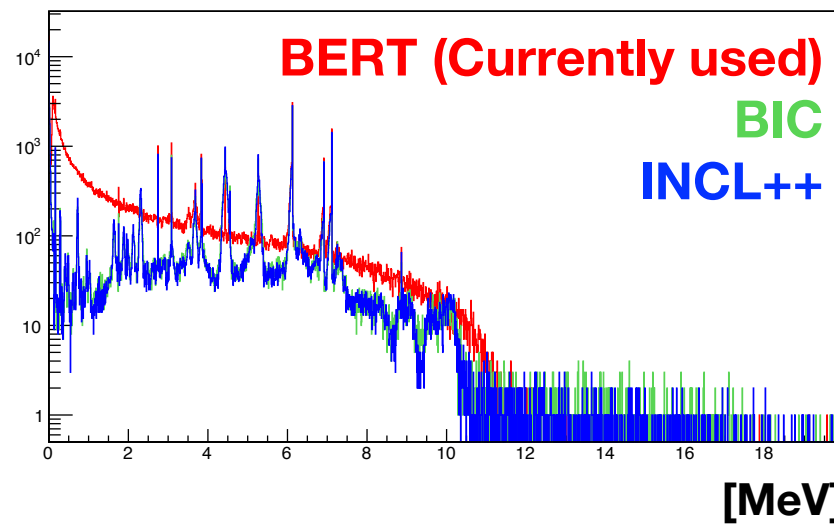
30 MeV

80 MeV

250 MeV

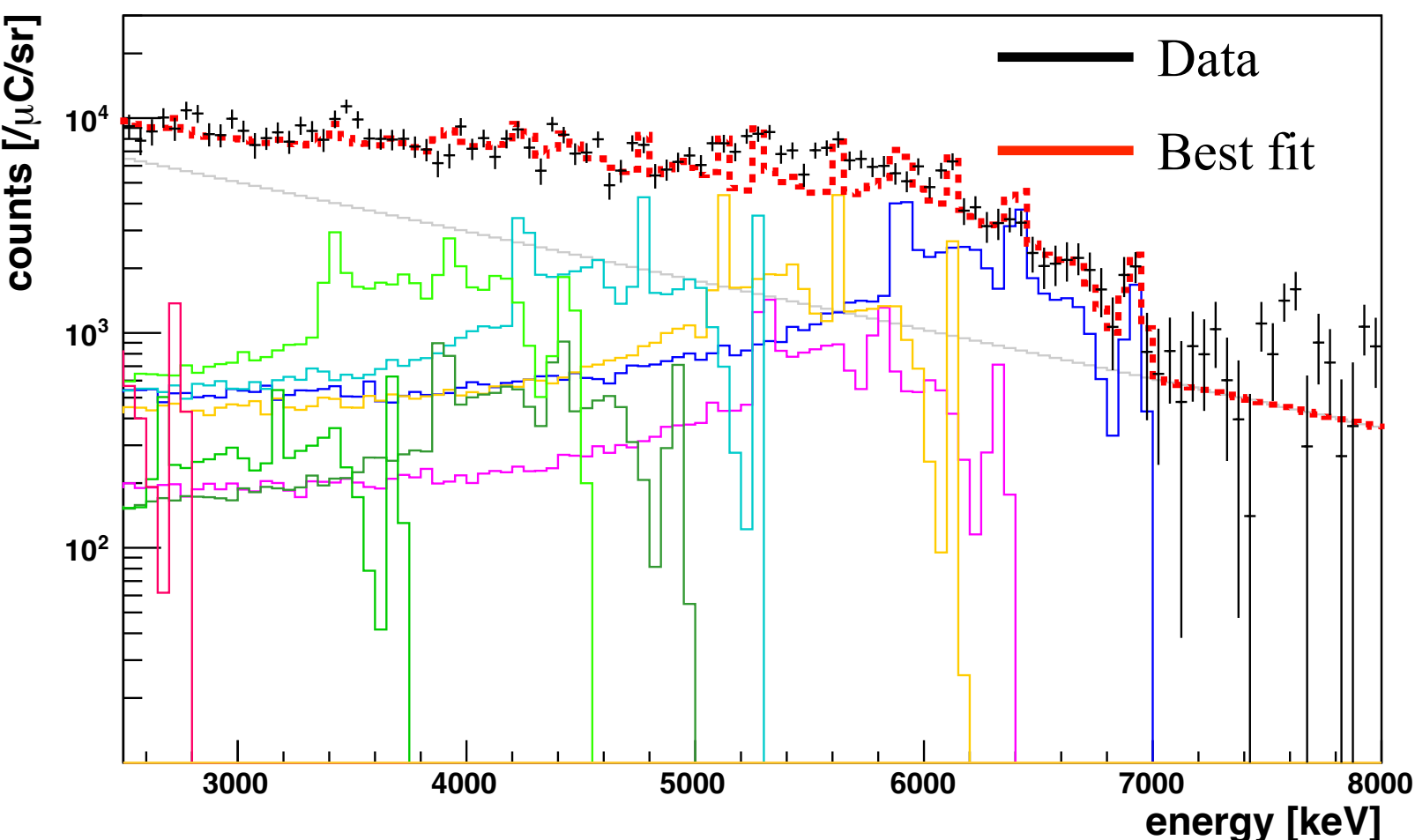


- これらの実験データを再現するようにモデルを修正  
→ 中性子・酸素原子核由来の不定性の削減

Energy of secondary  $\gamma$  (MC, true)

# フィッティング結果

- 用意したテンプレートにパラメータをかけて足し合わせる  
→ データを最もよく再現するパラメータセットを求める
- 高エネルギー側から、光電吸収ピークを用いて  $\chi^2$  を計算



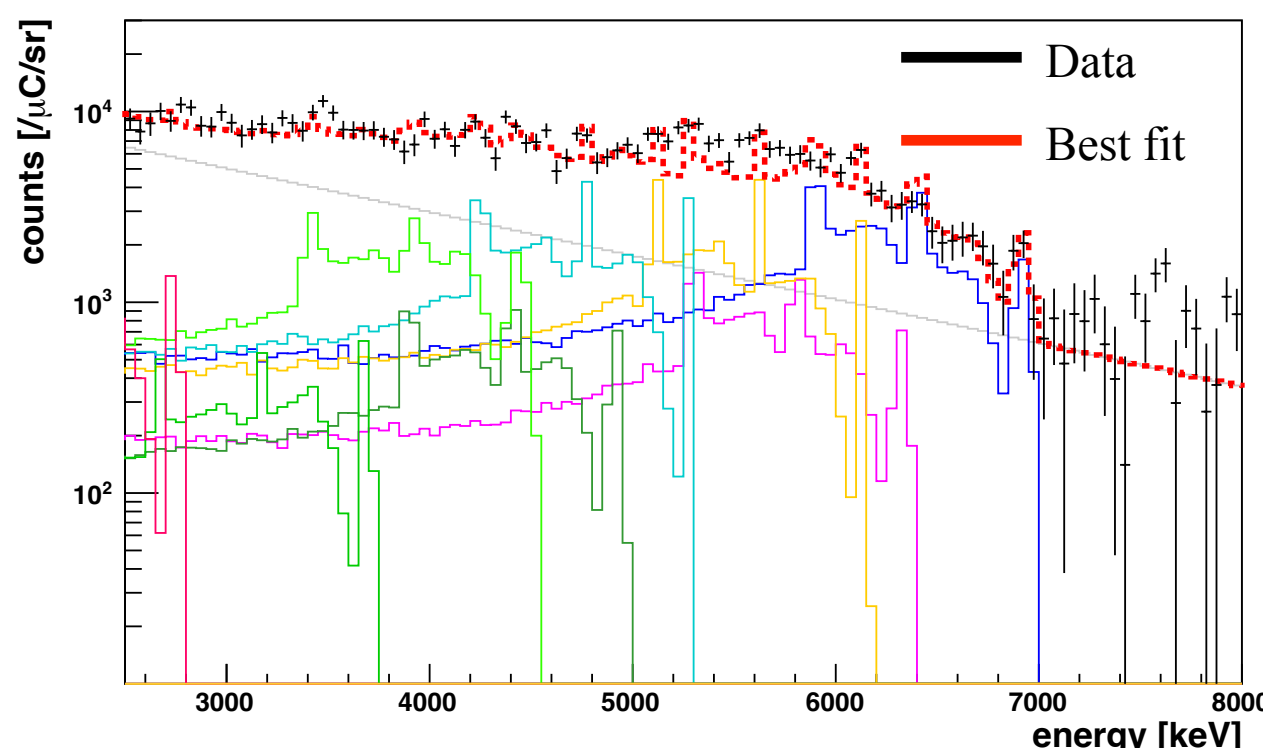
エネルギー [MeV]	6.32 MeVに対する強度
6.92	$2.96^{+0.35}_{-0.44}$
6.32	$1.00^{+0.37}_{-0.37}$
6.13	$2.23^{+0.60}_{-0.37}$
5.27	$2.35^{+0.63}_{-0.40}$
5.10	$0.00^{+0.33}_{-0.33}$
4.91	$0.63^{+0.33}_{-0.33}$
4.44	$2.08^{+0.38}_{-0.29}$
3.84	$0.00^{+0.13}_{-0.13}$
3.68	$0.33^{+0.15}_{-0.23}$
2.74	$0.56^{+0.27}_{-0.19}$

- 最も強いガンマ線：6.92 MeV
  - ▶  $^{16}\text{O}(\text{n}, \text{n}')^{16}\text{O}^*$  反応  
 $^{16}\text{O}^*$  の第三励起状態から放出される
- 各ガンマ線の生成断面積

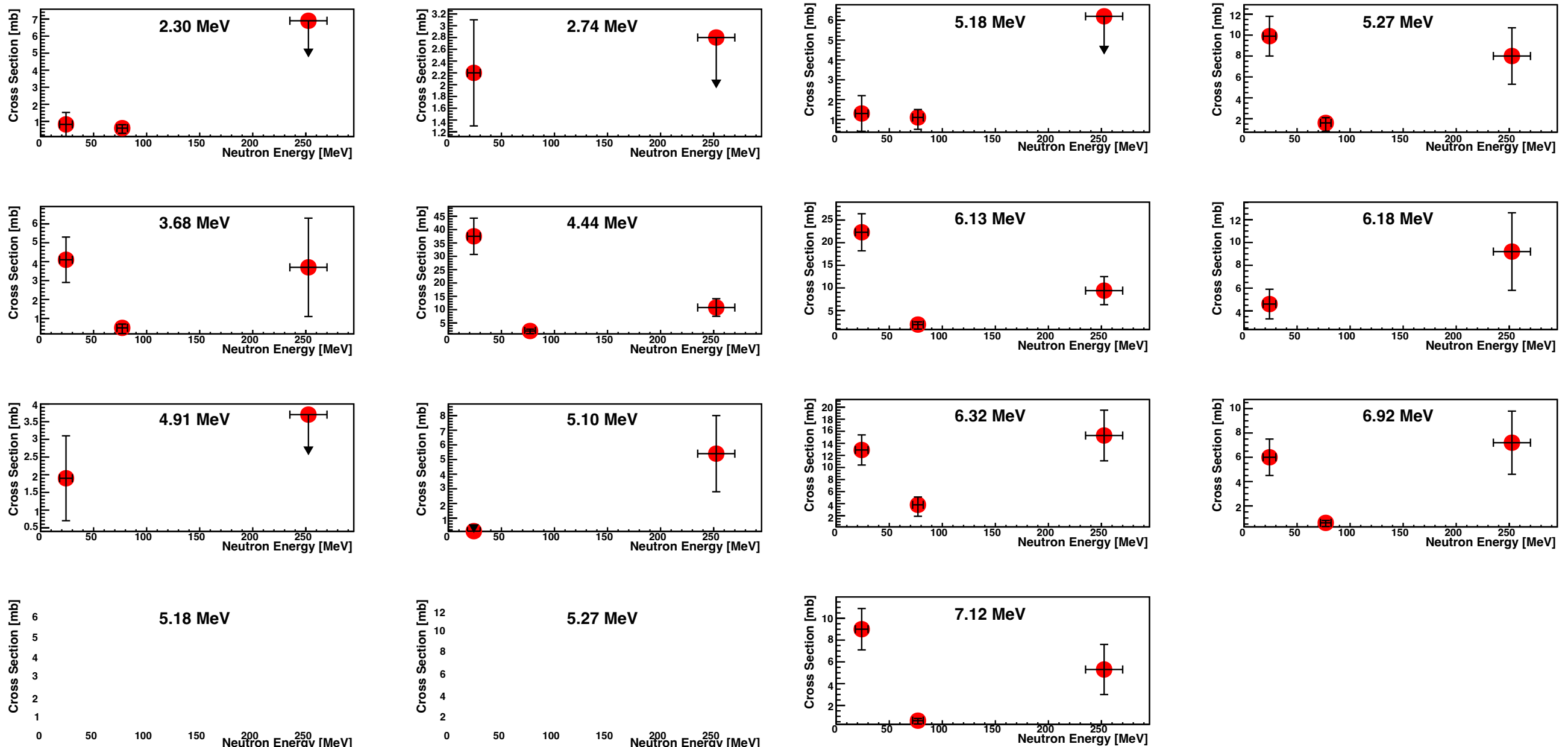
$$\sigma_{\gamma,j} = f_j \cdot \frac{N_{MCgenerated}}{\phi_n \cdot T}$$

$N_{MCgenerated} = 10^8$

$\phi_n$  : 中性子フラックス  
 $f_i$  : フィットで得たパラメータ  
 $T$  : 酸素原子核数



エネルギー [MeV]	6.32 MeVに対する強度
6.92	$2.96^{+0.35}_{-0.44}$
6.32	$1.00^{+0.37}_{-0.37}$
6.13	$2.23^{+0.60}_{-0.37}$
5.27	$2.35^{+0.63}_{-0.40}$
5.10	$0.00^{+0.33}_{-0.33}$
4.91	$0.63^{+0.33}_{-0.33}$
4.44	$2.08^{+0.38}_{-0.29}$
3.84	$0.00^{+0.13}_{-0.13}$
3.68	$0.33^{+0.15}_{-0.23}$
2.74	$0.56^{+0.27}_{-0.19}$



# まとめ

39

- 大気ニュートリノのNCQE反応は、SK-Gd実験でのSRN探索における主要な背景事象の一つである
- 特に、NCQE反応後の中性子と酸素原子核の反応に由来する不定性が大きい
- 中性子・酸素原子核反応を測定するE525実験が行われた
- 現在、250 MeV実験のデータ解析を進めている
- 中性子フラックスを算出した後、ガンマ線スペクトルをフィッティングして各ガンマ線の強度を求めた
- フィッティングの結果、最も強いガンマ線は酸素原子核由来の 6.92 MeVであり、非弾性散乱が支配的な反応であることが分かった
- これらの反応をシミュレーションに導入することで、中性子・酸素原子核反応由来の不定性の削減が期待される